Evolution of Cell-to-Cell Variability in Stochastic, Controlled, Heteroplasmic mtDNA Populations

Iain G. Johnston[1,*] and Nick S. Jones[2]

Populations of physiologically vital mitochondrial DNA (mtDNA) molecules evolve in cells under control from the nucleus. The evolution of populations of mixed mtDNA types is complicated and poorly understood, and variability of these controlled admixtures plays a central role in the inheritance and onset of genetic disease. Here, we develop a mathematical theory describing the evolution of, and variability in, these stochastic populations for any type of cellular control, showing that cell-to-cell variability in mtDNA and mutant load inevitably increases with time, according to rates that we derive and which are notably independent of the mechanistic details of feedback signaling. We show with a set of experimental case studies that this theory explains disparate quantitative results from classical and modern experimental and computational research on heteroplasmy variance in different species. We demonstrate that our general model provides a host of specific insights, including a modification of the often-used but hard-to-interpret Wright formula to correspond directly to biological observables, the ability to quantify selective and mutational pressure in mtDNA populations, and characterization of the pronounced variability inevitably arising from the action of possible mtDNA quality-control mechanisms. Our general theoretical framework, supported by existing experimental results, thus helps us to understand and predict the evolution of stochastic mtDNA populations in cell biology.

Introduction

Molecules of mitochondrial DNA (mtDNA) form dynamic evolutionary populations within cells, replicating and degrading according to cellular control signals.[1,2] mtDNA can vary due to mutation or artificial manipulation;[3] the proportion of mutant mtDNA in a cell is referred to as heteroplasmy. mtDNA encodes vital aspects of the bioenergetic machinery of eukaryotic cells; mtDNA variability can thus have dramatic cellular consequences, including devastating genetic diseases and numerous other conditions,[3] making a theoretical understanding of this complex evolutionary system important. Understanding the natural feedback control acting on mtDNA populations is also a vital step in the development of artificial approaches to control mitochondrial behavior with genetic tools.[4,5] Cell-to-cell variances of mtDNA copy number and heteroplasmy are of particular importance, owing to their implications for maternal transmission of dangerous mutations[6] and the manifestation of pathologies dependent on the range of heteroplasmies present in a tissue[7]—even a very small proportion of cells exceeding a heteroplasmy threshold can lead to pathologies.[8]

Stochastic behavior underlies much of cell biology and contributes to this cell-to-cell variability; cellular processes including gene expression,[9–11] DNA replication,[12] and mitochondrial and mtDNA dynamics[13–16] are subject to fundamentally stochastic influences. Variability in mitochondria can be a leading contributor to cell physiological behavior, making mitochondria an important target for explanatory stochastic models.[15] Existing studies have included stochastic modeling and numerical treatments of mitochondrial[17] and mtDNA populations, making quantitative progress with the assumption of specific control mechanisms.[1,14,18–20] Other theoretical studies have drawn on classical statistical genetics, notably including the well-known Wright formula,[21,22] to produce a description of partitioning of mtDNA populations at cell divisions, but the role of stochastic mtDNA dynamics between cell divisions is largely omitted. Although recent experimental studies are starting to shed light on cellular control of mtDNA,[14,16] a general theoretical framework is currently absent. Here we address this open question by constructing a general, bottom-up stochastic description of mtDNA populations subject to arbitrary cellular control mechanisms, providing analytic results for the predicted behavior associated with any mtDNA control mechanism, and adapting the classic Wright formula to account for and interpret stochastic mtDNA dynamics. Notably, our approach and results hold independently of the details of specific regulatory mechanisms underlying mtDNA feedback signaling, providing a general theoretical framework for control of stochastic mtDNA populations across different species and environments.

As we develop the theoretical framework to address mtDNA dynamics below, we will consider a set of applications of the theory, linking with existing experimental data from a variety of studies to validate our approach and obtain quantitative results and predictions on the processes governing mtDNA dynamics. We will focus on two questions arising from the study of mtDNA diseases: (1) how and at what rate does cell-to-cell heteroplasmy variance increase and (2) how selective pressure against a particular

[1]School of Biosciences, University of Birmingham, Birmingham B15 2TT, UK; [2]Department of Mathematics, Imperial College London, London SW7 2BB, UK
*Correspondence: i.johnston.1@bham.ac.uk
http://dx.doi.org/10.1016/j.ajhg.2016.09.016.

Box 1. Key Biological Findings from Our Mathematical Model

These results arise when the assumptions of our modeling approach hold: that cells are heteroplasmic, mtDNA replication and degradation are Poisson processes with the same rates for mutant and wild-type mtDNA, and feedback mechanisms depend only on the current state of the system. We justify these assumptions with reference to experimental data in the text and in Appendix A.

I. When mean copy numbers are constant, at least one variance (wild-type or mutant) increases linearly with time (Equations 8, 9, and 10).
II. When mean copy numbers are constant, heteroplasmy variance increases linearly with time with a rate that depends only on mtDNA copy numbers and the rate of mtDNA turnover, and not on any details of mechanism or signaling (Equation 12); many copy-number control mechanisms are therefore indistinguishable even from dynamical measurements of heteroplasmy (Figures 1 and 2).
III. Control applied through (1) biogenesis rates and (2) degradation rates induce comparable behavior in the cellular mtDNA population (Figure 1; Supplemental Data Section 2).
IV. A modified Wright formula (Equation 14; Figure 4) gives a general method to establish a quantitative link between observed normalized heteroplasmy variance $\langle h^2 \rangle'$ and observable (as opposed to effective) quantities (Figure 4).
V. Quality control does not guarantee the clearing or stabilization of mutant load and can induce substantial variance in wild-type mtDNA (potentially challenging cells with diminished populations; Figures 5 and 6).

mtDNA mutation affects cellular mtDNA populations. The single-cell measurements required to address these questions directly remain challenging: we aim to show that mathematical theory, appropriately validated and refined with available data, provides a powerful alternative route to make quantitative progress understanding this important behavior. Box 1 summarizes the central biological messages arising from development and analysis of our theory.

Material and Methods

We will consider mtDNA populations in cells that are heteroplasmic with two non-recombining haplotypes, though this treatment can readily be extended to more mtDNA types. We write a state with w wild-type mtDNAs and m mutant mtDNAs as $\{w,m\}$. We first consider the class of systems where both haplotypes are subject to the same degradation rate ν and the same replication rate λ, both of which may be general functions of both haplotype copy numbers. This model thus represents the situation where no direct selective difference exists between mutant and wild-type. This assumption holds for only some biological cases (see Burgstaller et al.[23] and references therein for a review of studies where mtDNA types segregate unevenly) and will be relaxed later. We also assume that cellular control is based only on the current state of the cellular mtDNA population and not its history. The dynamics governing the system then consist of a set of Poisson processes:

$$\{w,m\} \xrightarrow{w\lambda(w,m)} \{w+1,m\}, \qquad \text{(Equation 1)}$$

$$\{w,m\} \xrightarrow{m\lambda(w,m)} \{w,m+1\}, \qquad \text{(Equation 2)}$$

$$\{w,m\} \xrightarrow{w\nu(w,m)} \{w-1,m\}, \qquad \text{(Equation 3)}$$

$$\{w,m\} \xrightarrow{m\nu(w,m)} \{w,m-1\}. \qquad \text{(Equation 4)}$$

This formalism captures a wide range of models for mtDNA dynamics (see below). We will begin with the assumption that the system does not undergo cell divisions and has a stationary state in the population mean of both haplotype copy numbers, and we will write this steady state as $\{\tilde{w},\tilde{m}\}$. This initial picture is more appropriate for quiescent cell types or mtDNA "set points" than for the pronounced changes in mtDNA copy number that occur during development.[2,14] We will later generalize this picture to allow for arbitrary changes in copy number.

We will first consider general results from this formalism, applicable to a wide variety of possible cellular behaviors. We will then illustrate its application with a range of previously proposed and new feedback mechanisms.

Results

Copy-Number Variance with Stable Population Means

Any control mechanism of the form in Equations 1, 2, 3, and 4 (including manifestations of feedback control) can be represented to linear order by a Taylor expansion of its rates about $\{\tilde{w},\tilde{m}\}$ (the steady state exists by construction from our previous assumption):

$$\lambda(w,m) \simeq \beta_0 + \beta_w(w-\tilde{w}) + \beta_m(m-\tilde{m}), \qquad \text{(Equation 5)}$$

$$\nu(w,m) \simeq \delta_0 + \delta_w(w-\tilde{w}) + \delta_m(m-\tilde{m}). \qquad \text{(Equation 6)}$$

It will readily be seen that to support a stable population mean at $\{\tilde{w},\tilde{m}\}$, $\delta_0 = \beta_0$. Assuming that w and m can be written as the sum of a deterministic and a fluctuating component, we use Van Kampen's system size expansion to find a Fokker-Planck equation describing the behavior of w and m

governed by Equations 5 and 6.[24,25] From this equation we extract expressions for the time behavior of the mean and variance of w and m (see Supplemental Data Sections 1 and 2).

We show in Supplemental Data Section 4 that attempting to identify a stable state for population variances and covariance yields the condition

$$\frac{2\tilde{m}(\tilde{m}+\tilde{w})\beta_0}{\tilde{w}} = 0; \qquad \text{(Equation 7)}$$

hence, any population mean state in which mutant content $\tilde{m}$ is nonzero does not admit a stationary solution for variances, unless $\beta_0 = 0$. If $\beta_0 = 0$ then there is no further change to the system once steady state has been reached (no stochastic turnover occurs) and the system remains frozen thereafter. In other words, for a nonzero mutant population and nonzero mtDNA turnover, the variance of at least one mtDNA population will change with time.

The Fokker-Planck equation we derive can be used to compute the expected behaviors of $\langle w^2\rangle$ (wild-type variance), $\langle m^2\rangle$ (mutant variance), and $\langle wm\rangle$ (wild-type mutant covariance) for a given control mechanism. The variance and covariance solutions display some transient behavior, involving terms on the timescale $t' \equiv \exp(((\beta_m - \delta_m)\tilde{m} + (\beta_w - \delta_w)\tilde{w})t)$. Because, for stability, β_i are nonpositive and δ_i are nonnegative, t' is either a constant or an exponentially decaying function of time t. The expressions thus subsequently converge to linear trends for large t:

$$\langle w^2\rangle = F_1^{decay}(t') + \theta_1 t + \phi_1, \qquad \text{(Equation 8)}$$

$$\langle wm\rangle = F_2^{decay}(t') + \theta_2 t + \phi_2, \qquad \text{(Equation 9)}$$

$$\langle m^2\rangle = \underbrace{F_3^{decay}(t')}_{\substack{\text{transient}\\ \text{behaviour}}} + \underbrace{\theta_3 t + \phi_3}_{\substack{\text{long-term linear}\\ \text{behaviour}}}. \qquad \text{(Equation 10)}$$

The forms of the transient functions F_i^{decay} and the constants θ_i and ϕ_i are given in Supplemental Data Section 2 and are functions only of the difference between replication and degradation rates $(\beta_i - \delta_i)$, steady-state copy numbers $\tilde{m}$ and $\tilde{w}$, and mitophagy rate β_0. Furthermore, the structure of these expressions is such that for $\beta_0 \neq 0$ and nonzero w and m, at most one of the θ_i can be zero, $\theta_1 \geq 0$, and $\theta_3 \geq 0$. Thus, around the mean $(\tilde{w}, \tilde{m})$, *either wild-type variance or mutant variance or both increase linearly with time* (Box 1, I). As time continues, the increasing variance means that extinction of one mtDNA becomes increasingly likely; implications of this behavior are explored below.

The mathematical structure of the solutions only ever involves the *difference* between replication and degradation rates $(\beta_i - \delta_i)$, showing that *control of (1) biogenesis rates and (2) degradation rates induce comparable behavior in the cellular mtDNA population* (Box 1, III).

Heteroplasmy Statistics

As shown in Supplemental Data Section 5, a first-order Taylor expansion gives an approximation for the variance of $h = m/(w+m)$:

$$\langle h^2\rangle = \frac{\langle w\rangle^2\langle m^2\rangle + \langle m\rangle^2\langle w^2\rangle - 2\langle wm\rangle\langle w\rangle\langle m\rangle}{(\langle m\rangle + \langle w\rangle)^4}, \qquad \text{(Equation 11)}$$

and we can then use previously obtained expressions for $\langle w\rangle, \langle m\rangle, \langle w^2\rangle, \langle m^2\rangle, \langle wm\rangle$ to compute this approximate heteroplasmy variance. Neglecting transient terms and using $\langle w\rangle = \tilde{w}$ and $\langle m\rangle = \tilde{m}$ in Equation 11 gives, after some algebra,

$$\langle h^2\rangle = \frac{2\beta_0}{n}h(1-h)t; \quad \frac{\langle h^2\rangle}{\langle h\rangle(1-\langle h\rangle)} \equiv \langle h^2\rangle' = \frac{2\beta_0 t}{n}, \qquad \text{(Equation 12)}$$

where $n = \tilde{w} + \tilde{m}$, with $\tilde{w} = (1-h)n$ and $\tilde{m} = hn$; thus, h is (mean) heteroplasmy and n is (mean) total copy number (recall that $\beta_0 = \delta_0$ in steady state). In Equation 12 we have used normalized heteroplasmy variance $\langle h^2\rangle'$, accounting for the dependence of $\langle h^2\rangle$ on the magnitude of h; $\langle h^2\rangle'$ is the quantity most often reported in experimental studies.

In other words, when the system size expansion is valid (see below), for any control mechanism, *heteroplasmy variance in the copy number steady state increases linearly with time with a rate that depends only on the copy numbers of the system and the timescale of random turnover* (Box 1, II) (Equation 12 is independent of the β and δ terms in Equations 5 and 6). As we discuss later, this observation implies that many possible mechanisms could be responsible for the same observed trend in heteroplasmy variance, meaning that measurements of heteroplasmy variance alone, even if repeated at different time points, place only a limited mechanistic constraint on mtDNA dynamics.[14] In Supplemental Data Section 7, we discuss experimental strategies that can more efficiently discriminate between different control mechanisms.

Transient Behavior and Cell Divisions and Validity of the Expansion

To obtain analytic insight, we have thus far focused on modeling mtDNA behavior using the system size expansion when a steady-state assumption had already been applied. Transient behavior can also be explored by employing the system size expansion directly on the appropriate master equation, using the full expressions for $\lambda(w,m)$ and $\nu(w,m)$ (see Supplemental Data Sections 2 and 6). Relaxing the steady state assumption means that the ODEs describing variance behavior are analytically intractable for many forms of $\lambda(w,m), \nu(w,m)$. However, they can simply be solved numerically and, as shown in subsequent sections, well match stochastic simulation (which of course is numerically far more intensive). This

ODE approach fully accounts for non-equilibrium behavior—including transient relaxation, cell cycling, and so on—while the system size expansion remains appropriate (see below).

This analysis can readily be used to characterize the effect of partitioning mtDNAs at cell divisions. To compute the time behavior of variance where cell divisions occur at arbitrary times, we invoke a linear noise assumption,[24,25] first using the ODEs above to compute the variance behavior within one cell cycle. Partitioning rules for copy-number statistics are then applied, and the resulting post-partition statistics are used as the initial condition for a next phase of ODE solution. We here illustrate this process for binomial partitioning of mtDNAs to connect with recent studies in mice[14] and HeLa,[15] although with an appropriate choice of partitioning rules, this approach can be used to address any partitioning regime (for example, the sub-binomial case recently reported in fission yeast[16]). In the case of binomial partitioning, the appropriate partitioning rules are $\langle w\rangle \to \langle w\rangle/2, \langle m\rangle \to \langle m\rangle/2, \langle w^2\rangle \to \langle w^2\rangle/4 + \langle w\rangle/4, \langle wm\rangle \to \langle wm\rangle/4, \langle m^2\rangle \to \langle m^2\rangle/4 + \langle m\rangle/4$, following straightforwardly from the variance of a binomial distribution with $p = 1/2$. We will see below that this picture well describes the behavior of stochastic populations in dividing cells: hence, *the total variance contributions of turnover between divisions and partitioning at divisions can be modeled as a linear sum*, and the behavior of mechanisms across cell cycles is comparable to that within a cell cycle.

The results above hold for a nonzero mutant population. As copy-number variance increases, we expect extinction of one mtDNA type to become increasingly likely. To address this behavior, we must consider when the system size expansion itself, which is reliant on the validity of the linear noise approximation, holds. An important threat to this validity is a non-negligible extinction probability for one mtDNA type, whereupon a normal distribution no longer adequately models the copy-number distribution. Heuristically, this situation arises when, for example, $\sqrt{\langle m^2\rangle} \sim \langle m\rangle$. Another challenge arises due to the fact that, when λ and ν are functions of w and m, our linear theory is an approximation to the nonlinear dynamics that result. Highly nonlinear behavior (for example, pronounced discrete steps in rates occurring at critical copy numbers) will therefore not be perfectly captured, but the ability of our theory to reproduce simulation of the fully nonlinear dynamics (in Figures 1, 3, and 5 and Supplemental Data Section 3) suggests that the linear theory provides valuable insight into a wide range of biologically plausible behaviors. Treatments of fully nonlinear cases represent a substantial technical challenge that will be addressed in future work.

In cases where the validity of the system size expansion is challenged, the mean and variance of mtDNA populations are likely to be underestimated by the preceding analysis (see Supplemental Data Section 3), and the heteroplasmy variance will likely be overestimated, with the true increase in $\langle h^2\rangle$ with time gradually becoming sublinear. Fixation is also neglected by the deterministic version of the mean equations of motion, which allow only an asymptotic descent to zero. Thus, the more general statement of our findings are that (1) for the period when extinction of either type is unlikely, variances and covariances change linearly (after transients), (2) as extinction of one type becomes more likely due to this increased variance, the increasing trend continues but departs from those linear forms (in particular, the increase of $\langle h^2\rangle$ slows to become sublinear), and (3) when extinction of one type is almost certain, the system tends toward the behavior expected if only one type was present (ultimately stalling variance increase, as if $\tilde{m} = 0$ in Equation 7). The results we focus on in the remainder of this report can be viewed as describing the "quasi-stationary state" where extinction is negligible; further quantitative details can be derived using, for example, adaptations of the system size expansion that address extinction.[26]

Specific Control Mechanisms and Comparison with Simulation

The previous results make no assumptions about the specific form of control applied to the mtDNA population, other than the fact that it depends only on current state and is manifest through the rates of Poissonian replication and degradation that are equal for both mtDNA species (and can be described with the system size expansion, as discussed above). We can exploit the generality of the preceding formalism to obtain results for any given (feedback) control mechanism, defined by a specific form of $\lambda(w,m)$ and $\nu(w,m)$ in Equations 1, 2, 3, and 4.

We first consider the well-known "relaxed replication" model,[1,19] which involves stochastic mtDNA degradation, coupled with mtDNA replication that is physically modeled as a deterministic process. We propose that, if degradation is regarded as a stochastic process (due to its microscopic reliance on complicated processes and colocalizations in the cell), picturing replication (which also relies on complicated interactions on the microscopic scale) as a stochastic process leads to a consistent stochastic generalization (see Appendix A). The corresponding model has exactly the same expressions for rates as in Capps et al.[1] (type A in Figure 1A), but replication rate is now interpreted as the rate of a stochastic, rather than a deterministic, process.

We also introduce several other models for mtDNA control to consider a range of potential functional forms, including differential and ratiometric control based on a target wild-type copy number, an absence of any feedback control, and others (types B–G in Figure 1A). The presence or absence of w and m in these expressions reflects what quantity is being sensed by the cell (wild-type mtDNA alone, mutant mtDNA alone, or a combination of the two). We further note that this general formalism can also incorporate physical constraints on the mtDNA

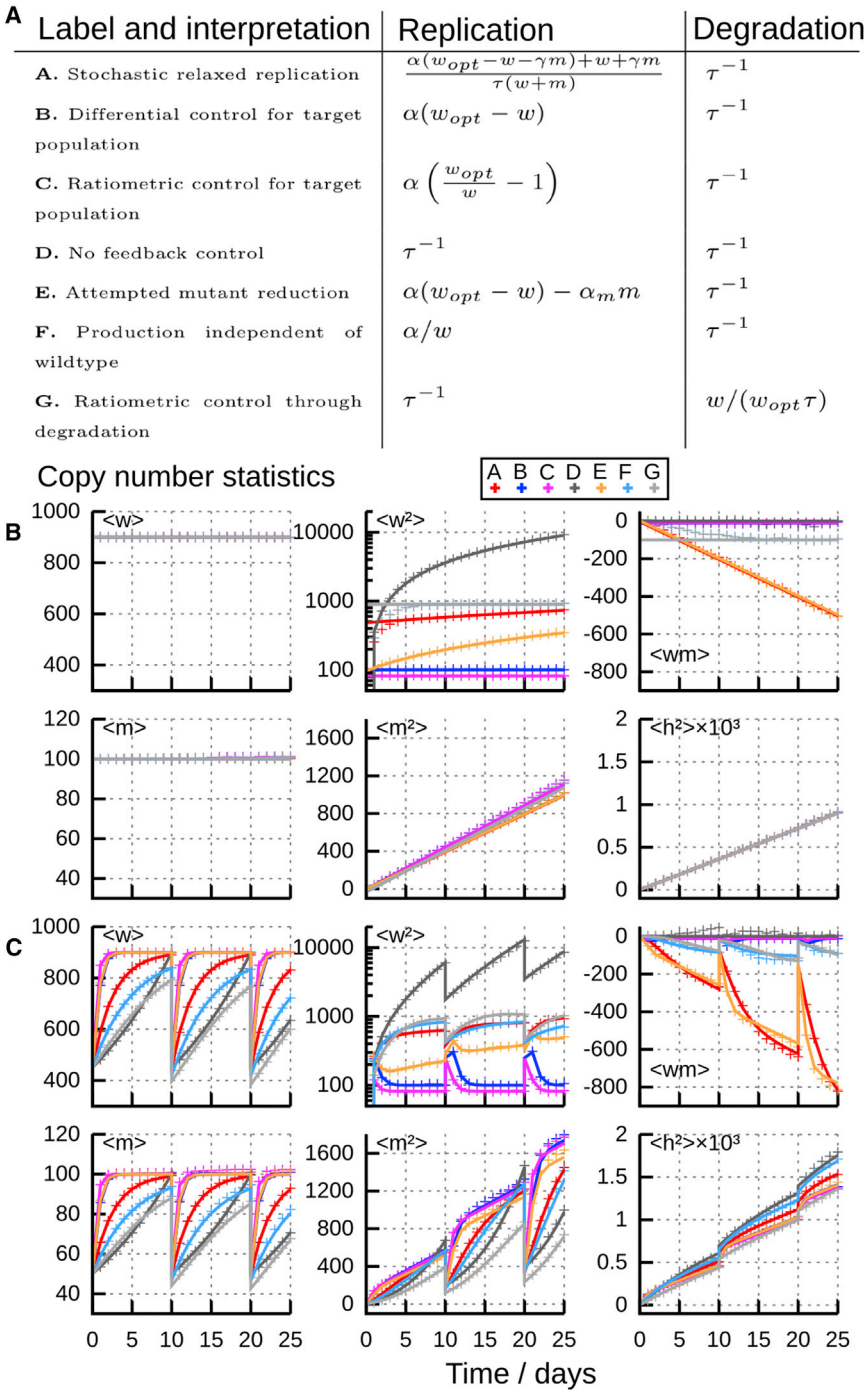

Figure 1. Behavior of Different Specific Control Mechanisms

All control mechanisms have at least one population with time-increasing variance and so have increasing heteroplasmy variance; mean heteroplasmy $\langle h \rangle$ remains constant through these simulations.

(A) Replication $\lambda(w,m)$ and degradation $\nu(w,m)$ rates for model control mechanisms explored in the text, from existing studies and newly proposed here.

(B and C) Copy number and heteroplasmy moments with time for these control mechanisms, (B) in the absence of cell divisions and (C) with binomial cell divisions every 10 days. Analytic results (lines; full expressions in Supplemental Data Section 3) match stochastic simulation (crosses) throughout. Parameters used are chosen to support the same steady state ($\tilde{w}=900, \tilde{m}=100$) and with a turnover timescale of $\tau = 5$ days. Other parameters: $\gamma = 0, \alpha_m = 0.001, \alpha = 2$ (except for models B, E, and F, for which $\alpha = 0.002, 0.002, 200$ respectively); 10^5 stochastic simulations used.

population. For example, the hypothesis that mitochondrial *concentration* is controlled between cell divisions[15] (recently confirmed in fission yeast[16]) could correspond to w_{opt}, the "target" mtDNA number, being a linear function of cell volume in the models above, or could arise through passive birth-death dynamics (model D) with control implemented at the cell division stage (see previous section). Interpretations of these control mechanisms in terms of cellular sensing and the language of stochastic population processes are given in Supplemental Data Section 3.

Figure 1B illustrates the application of our analysis to these example control mechanisms in the absence of cell divisions. The close agreement between stochastic simulation and analytic results in steady state demonstrates the ability of our general theory to describe a wide range of different potential cellular control mechanisms. The long-term linear increases in one or both mtDNA variances are clear (Box 1, I), and trajectories of $\langle h^2 \rangle$ with the same steady state and turnover timescale are identical (Box 1, II). Figure 1C, including cell divisions, demonstrates close agreement between ODE solutions and stochastic simulation, further showing that the linear noise treatment successfully captures stochastic behavior over cell divisions. The close similarity of $\langle h^2 \rangle$ trajectories across divisions is a consequence of their aforementioned identity in steady-state conditions with no cell divisions (Figure 1B); the slow divergence is due to differences in mechanism behavior away from the steady state.

Applications I: Heteroplasmy Variance Increases at Constant Mean Copy Number

The increase of heteroplasmy variance $\langle h^2 \rangle$ with time is of profound importance in determining the inheritance and onset of mtDNA diseases. Because disease symptoms often manifest only when heteroplasmy exceeds a certain

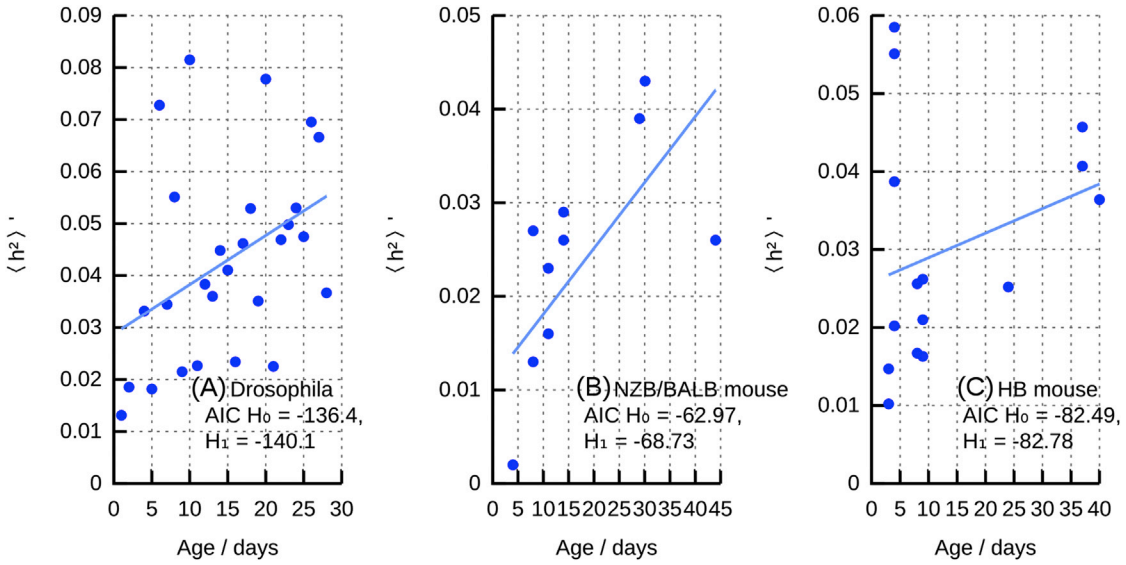

Figure 2. Experimental Support for Linear $\langle h^2 \rangle$ Increase
Normalized heteroplasmy variance $\langle h^2 \rangle'$ in model organism germlines over time (points); lines show maximum-likelihood linear fit for $\langle h^2 \rangle$ as a function of time. Insets give Akaike information criterion (AIC) values for $\mathcal{H}_0$ ($\langle h^2 \rangle'$ is constant) and $\mathcal{H}_1$ ($\langle h^2 \rangle'$ increases linearly with time). Model organism and reference(s): *Drosophila*[27] (A), NZB/BALB mice[28,29] (B), and HB mice[14] (C).

threshold,[7] increasing heteroplasmy variance with time can lead to pathologies even if mean heteroplasmy does not change (because a higher cell-to-cell variance implies a greater probability of a given cell exceeding a threshold).[14]

We sought experimental evidence to support the linear increase of $\langle h^2 \rangle$ predicted by our theory. Time course measurements of single-cell heteroplasmy values remain limited; we identified results from the *Drosophila* germline[27] and in the mouse germline for the NZB/BALB model[28,29] and the HB model.[14] For these data, we compared the ability to fit the data of a null model involving constant $\langle h^2 \rangle'$ ($\mathcal{H}_0 : \langle h^2 \rangle' = \alpha + \varepsilon$, where α is a constant) and an alternative model ($\mathcal{H}_1 : \langle h^2 \rangle' = \alpha + \beta t + \varepsilon$), where $\langle h^2 \rangle'$ changes linearly with time as our theory predicts (Equation 12; Box 1, II). Using the Akaike information criterion (AIC) and assuming normally distributed noise on mean $\langle h^2 \rangle'$ ($\varepsilon \sim \mathcal{N}(0, \sigma^2)$, an assumption consistent with our linear approximation but which can be further refined as in Wonnapinij et al.[29]), we found that the alternative, time-varying model was favored in all cases, providing support for our theory (Figures 2A–2C).

These results are quantitatively consistent with a previous study on the dynamics of heteroplasmy variance during the mtDNA bottleneck in mice[14] where a mechanism involving random mtDNA turnover and random mtDNA partitioning at cell divisions was found to best explain experimental observations. mtDNA in mice and rats often has a half-life of 10–100 days.[23] This corresponds to $\beta_0 = \delta_0 = \log 2 / t_{1/2} = 0.03 - 0.003$ day^{-1} and $\tau = t_{1/2}/\log 2 = 5 - 50$ days. In Figure 1 we show the patterns of copy number and heteroplasmy means and variances for $\tau = 5$ days and 10^3 mtDNA molecules per cell under different specific control strategies. The increase of $\langle h^2 \rangle$ from 0 to 10^{-3}, corresponding for $h = 0.1$ to an increase in $\langle h^2 \rangle'$ from 0 to 0.011, matches the scale of change observed in the mtDNA bottleneck (though the bottleneck is complicated by changing population size n and compensatory changing turnover β_0).[14] Previous work has shown that the case with no feedback (D in Figure 1) describes well the behavior of mtDNA with cell divisions in mouse development.[14] In Appendix A we discuss further connections with previous theoretical studies; experimental cell-to-cell measurements in more quiescent cell types, although currently lacking, will provide valuable further tests of our theory.

mtDNA Turnover in the Wright Formula

Powerful existing analyses of mtDNA population variance[22,29] with widespread influence[3] have drawn upon a classical theory by Wright (and Kimura)[21,30] describing stochastic sampling of a population of elements between generations. The resulting expression for expected heteroplasmy variance is the well-known equation sometimes referred to as the Wright formula (though other equations also bear this name):[3,22]

$$\langle h^2 \rangle' = 1 - \left(1 - (2n_e)^{-1}\right)^g, \qquad \text{(Equation 13)}$$

where n_e is an effective population size and g is a number of generations. The mapping of this effective theory to the complicated mtDNA system is valuable to develop intuition but cannot capture the detailed dynamics of individual mtDNA molecules, due to assumptions (see Appendix B) that mean the effective parameters of the theory (n_e and g) cannot generally be interpreted as biological observables,[22,31] preventing quantitative analyses of mechanisms and dynamics.[3] In particular, n_e does not generally correspond to a minimum mtDNA copy number (see

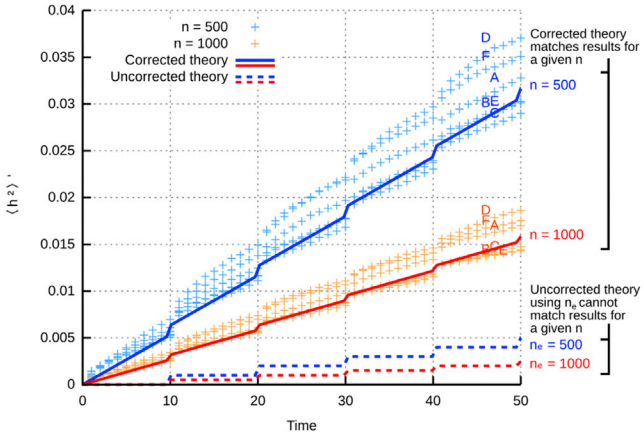

Figure 3. Correcting the Wright Formula to Include mtDNA Turnover and Connect to Biological Observables
Application of the Wright formula Equation 13 to stochastic mtDNA populations subject to division is only semiquantitative: the Unadjusted Theory lines (dashed) for given effective population sizes n_e do not describe the behavior of simulations of mtDNA populations of that size (crosses). Correcting for mtDNA turnover with Equation 14 quantitatively connects Theory lines (solid) and simulation (crosses); further improvement can be achieved using the ODE approach in Figure 2.

Appendix B), and, being a genetic rather than a physical parameter, "is unlikely ever to correspond closely to the number of anything."[31]

The Wright formula, however, does accurately describe the heteroplasmy variance due to binomial sampling of $2n_e$ real elements at cell divisions for an observable population size, and, as seen in the previous section, the additional effect of mtDNA turnover based on observable values can be included as an extra linear contribution. In general, this term will depend on the dynamics controlling the mtDNA population and can easily be calculated via the ODE approach above (Figure 1).

In the case where no systematic change in mtDNA population size occurs with time, we can use the observation that $\langle h^2 \rangle$ trajectories are often comparable across a variety of different possible cellular control mechanisms (and identical in the steady state; Figure 1 and Equation 12) to produce a simple approximate description linking $\langle h^2 \rangle'$ to observables. The simple steady-state behavior is given by Equation 12. To construct an approximation, we use a simple estimate of mean population size over a cell cycle, writing $n' = 3/2n$, where n is the mtDNA population size immediately after division and n' thus gives a population size "average" over the changes within a cell cycle. Using the above analysis with $w_0 = (1 - \langle h \rangle)n'$, $m_0 = \langle h \rangle n'$ (representing the "average" populations of wild-type and mutant mtDNA), and $\beta_0 = 1/\tau$ (so that τ is the timescale of mtDNA degradation), the corresponding expression in terms of h and n is then given by a "turnover-adjusted" Wright formula (see Appendix B):

$$\langle h^2 \rangle' = 1 - \left(1 - (2n)^{-1}\right)^g + 4t \Big/ (3n\tau), \qquad \text{(Equation 14)}$$

where g is the number of cell divisions that have occurred and t is the amount of time that has expired since an initial state with $\langle h^2 \rangle' = 0$. This expression is subject to the conditions for system size expansion validity described above; thus, as fixation probability increases, the increase of $\langle h^2 \rangle'$ will drop below this prediction.

Figure 3 illustrates the agreement between Equation 14 and stochastic simulation for the range of control mechanisms we consider under different population sizes and heteroplasmies. It is worth reiterating that more exact solutions for a given control mechanism can easily be computed using the preceding ODE approach, and stochastic analysis can also be used to quantitatively describe the effects of more specific circumstances (for example, the systematically varying population size through the mtDNA bottleneck[14]). In the case of no such systematic variation, and, crucially, *if the Poissonian model of Equations 1, 2, 3, and 4 holds, then Equation 14, a modified Wright formula, represents a simpler, approximate way to establish a quantitative link between observed normalized heteroplasmy variance* $\langle h^2 \rangle'$ *and observable quantities* (Box 1, IV), i.e., n (mtDNA copy number immediately after division), g (number of cell divisions), and τ (timescale of mtDNA turnover).

Applications II: Linking Physical and Genetic Rates with the Modified Wright Formula

The Wright formula is traditionally used to compare a heuristic, effective "bottleneck size" across experimental systems (for example, in studies of different organisms[22] and of human disease[32]). In its uncorrected form, this bottleneck size can only be semiquantitatively treated—bottleneck sizes can be ranked, but absolute values and differences cannot be straightforwardly interpreted. Our adaptation allows us to use this formula to connect the rates of physical subcellular processes with the resulting rates of genetic change.

To illustrate this connection, we focus on a particular period during mouse development. Between 8.5 and 13.5 days post conception (dpc) in the developing mouse germline, cell divisions occur with a period of about 16 hr,[33] giving $g = 7$ or 8 cell divisions in this period (of length $t = 5$ days). Copy-number measurements during this period show that the mean total number of mtDNA molecules per cell remains of the order of $n = 2{,}000$ (Figure 4A).[28,34,35] During this period, heteroplasmy variance $\langle h^2 \rangle'$ increases on average (but with substantial variability) from around 0.01 to 0.02 (Figure 4B).[28,36] Figure 4B shows a best-fit line to $\langle h^2 \rangle'$ data, with slope 1.52×10^{-3} day^{-1} (5%–95% confidence intervals $(1.11–1.92) \times 10^{-3}$ day^{-1}).

We can use these measurements in conjunction with the turnover-adjusted Wright formula (Equation 14) to obtain estimates for the rate of mtDNA turnover during this period. Using Equation 14 with the best-fit $\langle h^2 \rangle' = 1.52 \times 10^{-3} \times 5 = 7.6 \times 10^{-3}$, and $g = 7$ divisions, $n = 2{,}000$ mtDNA molecules, $t = 5$ days gives the resulting

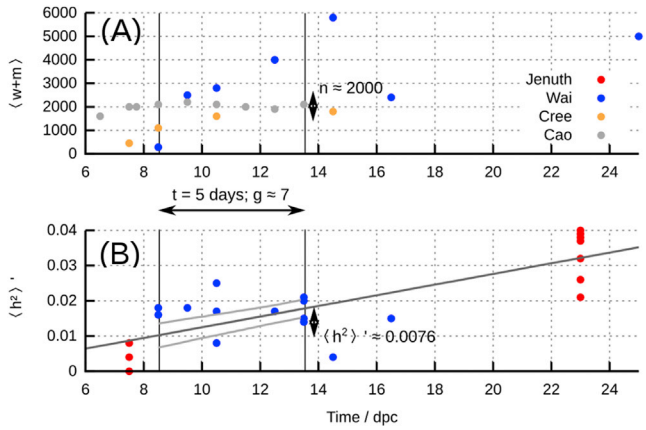

Figure 4. Using the Adapted Wright Formula to Estimate mtDNA Turnover

(A) mtDNA copy number n, taken to correspond to $\langle w+m \rangle$, in the mouse germline during development. Data from several existing studies, referred to by first author.[28,34–36]

(B) Normalized heteroplasmy variance $\langle h^2 \rangle'$ in this time period (points). Dark gray line is the mean inferred increase (which is linear, in agreement with our theoretical predictions, as in Figure 3). Light gray lines give the 95% confidence intervals in the 8.5–13.5 dpc window, from a linear model fit. Values used in the turnover-adjusted Wright formula (Equation 14) are given.

estimate $\tau \simeq 0.57$ days (5%–95% confidence intervals 0.43–0.88 days, using the same values for n, g, t) for the characteristic timescale of mtDNA degradation. This increase in mtDNA turnover (relative to the $\tau \simeq 5-50$ day timescale in differentiated tissues[23]) in the germline during this developmental period matches quantitative results from a more detailed study of the bottleneck reporting τ within the range 0.38–2.1 days (based on posteriors for $\nu = 1/\tau$ between 0.02 and 0.11 hr^{-1})[14] and illustrates how a suitable mathematical model can be used to estimate biological quantities that are challenging to directly address with experiment.[37]

Influence of Mutations, Replication Errors, and Selective Differences: Quality Control of Replication Errors

Our approach is easily generalized to include other processes than those described by Equations 1, 2, 3, and 4: in Supplemental Data Section 6 we demonstrate that adding and changing appropriate processes allows us to analyze the effects on mtDNA mean and variance due to de novo mutations, replication errors, and multiple selective pressures. Our approach can be thus used to characterize variability arising from selection and mutation under any control mechanisms, without requiring stochastic simulation.

We can use this ability to explore a particular scientific question: if mtDNA replication errors occur and the cell attempts to clear the resulting mutant mtDNA through selective quality control, how do cellular mtDNA populations change? To investigate this question, we introduce the process $\{w,m\} \overset{\mu w}{\to} \{w,m+1\}$ (replication errors—leading to the production of a new mutant mtDNA—occurring with rate μ) and reparameterize Equation 4 as $\{w,m\} \xrightarrow{(1+\varepsilon)m\nu(w,m)} \{w,m-1\}$ (an increase of ε in mutant degradation rate compared to wild-type degradation). We thus model the situation where replication errors arise and the cell attempts to clear them through quality control, while a control strategy for mtDNA populations is also in place.

Figure 5 illustrates the mean and variance of w and m in two different cases, distinguished by the relative magnitude of the selective difference (ε) and error rate (μ). This ratio is crucial in determining whether mutant mtDNA is cleared or increased: Figure 5A shows that mutant is cleared when $(1+\varepsilon\nu) \gg \mu$ (selection is sufficiently strong to overcome errors), but when selective difference ε is insufficiently high, mutant mtDNA mean and variance (and heteroplasmy) increase with time. In both cases, we also observe substantial differences in mtDNA behavior depending on the control model in place. Control models lacking an explicit target copy number (D, no feedback; F and G, immigration-like) experience substantial increases in wild-type variance while mutant is being removed. Models involving a target wild-type copy number and weak or no coupling to mutant mtDNA (B, C, E) admit an order-of-magnitude lower increase in wild-type variance as mutant is cleared. Relaxed replication (model A), which combines a target copy number with a strong coupling between mutant and wild-type mtDNA, displays an intermediate increase on wild-type variance as mutant is cleared.

Theoretical approaches that consider only the mean behavior of mtDNA populations (Figure 5A) cannot account for this cellular heterogeneity and the important fact that quality control acting to remove mutant mtDNA can also induce variability in wild-type mtDNA (Figure 5B). The action of quality control may therefore yield a subset of cells with wild-type mtDNA substantially lower than the mean value across cells—potentially placing a physiological challenge on those cells where wild-type mtDNA is decreased. In addition to the important point that the simple presence of quality control does not guarantee the clearing or stabilization of mutant load, we thus find that *quality control may have substantial effects on wild-type as well as mutant mtDNA if cellular control couples the two species* (Box 1, V).

Applications III: Variance Induced through Mutant Clearing

The A>G mutation at position 3243 in human mtDNA is the most common heteroplasmic pathological mtDNA mutation, giving rise to MELAS (mitochondrial encephalomyopathy, lactic acidosis, and stroke-like episodes), a multi-system disease. The dynamics of c.3243A>G heteroplasmy are complex and tissue dependent; its behavior in blood has been characterized in particular detail using a fluorescent PCR assay for heteroplasmy[38] in a way that

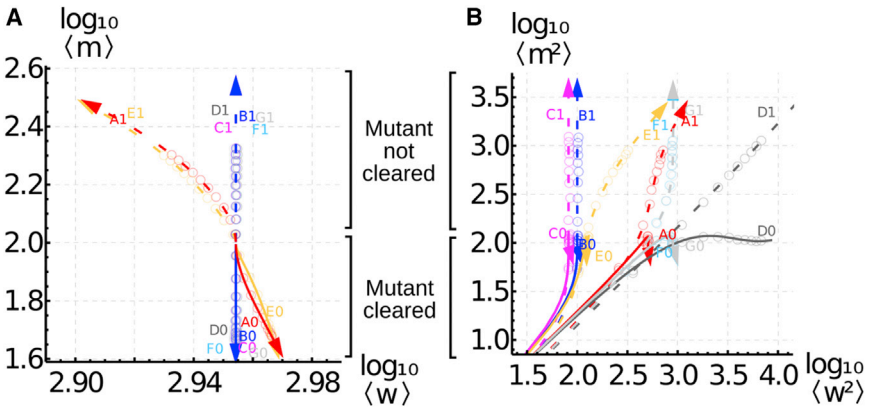

Figure 5. Variability in Quality Control Clearing of Mutants from Replication Errors

Co-evolution of (A) means and (B) variances of mutant m and wild-type w mtDNA in cells where replication errors occur. Solid lines (downward trajectories; labels A0–F0) give the case where quality control is sufficiently strong to clear the resulting mutant molecules (hence decreasing $\langle m \rangle$ in A); dashed lines (upward trajectories; labels A1–F1) give the case where quality control cannot clear mutants (hence increasing $\langle m \rangle$). Colors and labels correspond to different control models (see text and Figure 2). Points show stochastic simulation. Importantly, regardless of the success of quality control in clearing mutants, wild-type mtDNA variability $\langle w^2 \rangle$ can increase substantially during the action of quality control (rightward movement in B), and some strategies lead to order-of-magnitude differences in this increase (starred arrow).

allows us to explore our theoretical predictions about mtDNA statistics with mutant clearing.

Pyle et al.[38] took two blood samples, several years apart, from human patients, and quantified c.3243A>G heteroplasmy (h) and mean mtDNA copy number per cell for both samples. Although single-cell data are not presented in the publication, progress can be made with the averaged quantities. A strong decrease in (h) with time is observed for all patients, confirming that mutant mtDNA is being cleared (Figure 6A). The behavior of total mtDNA molecules per cell ($w + m$) is less consistent, with a range of large increases and moderate decreases in total number. As shown in Figures 6B and 6C, patient-to-patient variance in both w and m increases with time in conjunction with h decreases.

Although the measurements in Pyle et al.[38] are averages over groups of cells, an approximate quantitative comparison of these data with the predictions of our theory can be made. In the spirit of "back-of-the-envelope" calculations,[39] we estimate that each sample of cells giving rise to a measurement corresponds to approximately 10^3 cells (see Supplemental Data Section 8). Then, using an estimate of $\tau = 5$ days (by comparison with other mammalian species, as above), we find that a selective pressure of $\varepsilon_8 \simeq 1.2\times10^{-4}$ day^{-1} matches the observed decrease in heteroplasmy, corresponding, for example, to a decrease from 0.15 to 0.14 over 8 years, as in Figure 6A. Solving the ODEs resulting from this system, using control model D as the simplest case, predicts increases in cell-to-cell copy-number variance of approximate magnitude $\langle w^2 \rangle \sim 10^5$ and $\langle m^2 \rangle \sim 2\times10^4$ over 8 years. We can translate these cell-to-cell values into the variance expected across samples of cells by dividing by the number of samples (taken as 10^3 as above). The resulting variance corresponds, for example, to expected standard deviations in wild-type and mutant copy number after 8 years of 10.0 and 4.0, respectively, for a sample with $\langle w \rangle = 85$ and $\langle m \rangle = 15$ (consistent with the increasing spread of values in Figures 6B and 6C). We used the Kolmogorov-Smirnov test to test the alternative hypotheses that the experimentally observed $\langle w \rangle$ and $\langle m \rangle$ at the later time point differed from those predicted by our model; no test yielded $p < 0.05$ (see Supplemental Data Section 8). Of course, an absence of support for an alternative hypothesis cannot be taken as support for a null hypothesis, but shows that the existing experimental data are not incompatible with our model.

The observations in Figure 6 support the predictions made in Figure 5, where mutant load is decreased but variance in wild-type copy number (and mutant copy number) increases. The bottom-left quadrant of Figure 5B shows that different control mechanisms display similar initial behavior; follow-up studies on these subjects could be used to distinguish possible mechanisms for mtDNA control. For example, if the rate of wild-type variance increase decreases over time, models B, C, and E are more likely; if wild-type variance continues to increase, models A, D, F, and G are more likely. More detailed model discrimination based on the time behavior of w and m variances are possible (Figure 1) and can be performed using statistical methods accounting for mean and variance behavior.[29,40]

Discussion

A general, bottom-up theory has been produced to describe the time behavior of cell-to-cell variance in mtDNA populations subject to controlled biogenesis and/or degradation, mutation, selection, and cell divisions. This theory is based around the microscopic behavior of mtDNA molecules, allowing a hitherto absent connection between widely used "effective" statistical genetics approaches (Equation 13) and measurable biological quantities, and motivating experiments to further elucidate the mechanisms acting to control mtDNA (described in Supplemental Data Section 7). We have shown that the predictions of this theory agree

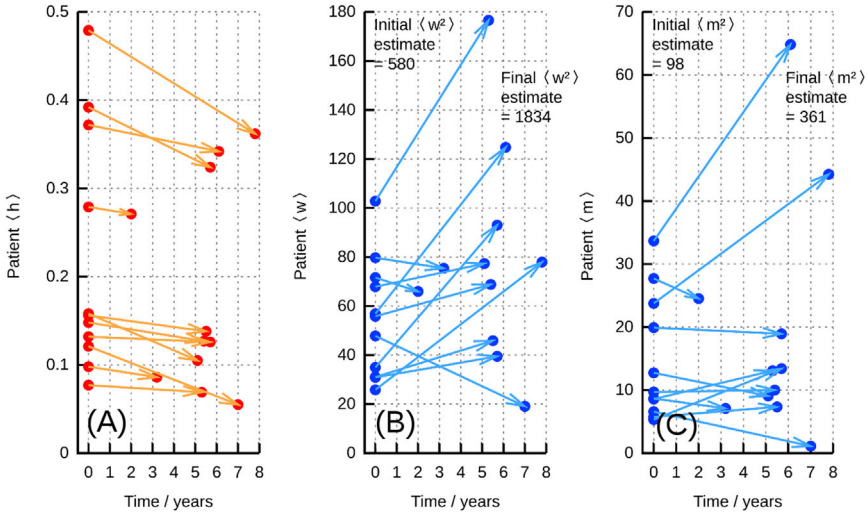

Figure 6. mtDNA Evolution in MELAS Patients from Pyle et al.[38]
(A) Changes in mean heteroplasmy $\langle h \rangle$ between two samples from patient blood, showing a general decrease in $\langle h \rangle$ over time.
(B) Changes in mean cellular wild-type content w between these samples.
(C) Changes in mean cellular mutant content m.
In both (B) and (C), an overall increase in variance over time is observed: hence $\langle w^2 \rangle$ and $\langle m^2 \rangle$ increase while $\langle h \rangle$ decreases, consistent with Figure 6.

with experimental observations of mixed mtDNA populations and that the application of appropriately validated mathematical theory allows us to make estimates of important biological quantities that remain challenging to directly address with experiments. Our theory describes the cell-to-cell variability in mtDNA populations and thus provides a framework with which to understand the inheritance and onset of mtDNA diseases.[6,14]

Our theoretical platform unifies several existing modeling approaches that have driven advances in the study of mtDNA populations. We have specifically demonstrated that the "relaxed replication" model[1,19,34] (our model A), simple birth-death models[14,20] (our model D), and cellular controls based on homeostatic principles[15,16] (our models B, C, and G) can naturally be represented within our framework. As a result, analytic expressions for the expected behavior of heteroplasmy variance and other population statistics can readily be extracted for these and other mtDNA models (see Supplemental Data Section 3), allowing the detailed characterization of mtDNA dynamics, including the probability of crossing disease thresholds,[7] which can be computed from heteroplasmy statistics.[14] We have also used the theoretical ideas developed herein to refine a widely used model for mtDNA populations of changing size (the Wright formula), explicitly connecting it with cellular processes and allowing a link between physical and genetic quantities (Equation 14, Figure 4).

Further, our theory also describes the dynamics of heteroplasmy change with time in the presence of selective pressure for one mtDNA type. Given an initial heteroplasmy h_0 and a selective pressure β (positive β corresponding to positive selection for the mutant mtDNA type), we find (see Supplemental Data Section 5) that heteroplasmy evolves according to:

$$h = \frac{1}{1 + \frac{1 - h_0}{h_0} e^{-\beta t}}. \qquad \text{(Equation 15)}$$

This behavior immediately motivates a transformation, allowing the evolution of heteroplasmy to be compared across different starting values h_0:

$$\Delta h' \equiv \beta t = \log\left(\frac{h(h_0 - 1)}{h_0(h - 1)}\right), \qquad \text{(Equation 16)}$$

allowing, as in our previous work,[23] heteroplasmy results from different biological samples to be compared together, accounting for different initial heteroplasmies (in other words, the same selective pressure will produce the same $\Delta h'$ regardless of h_0).

It is likely that control mechanisms found in biology have nonlinear forms (for example, sigmoidal response curves are common in cellular signaling). We have shown that a linearization satisfactorily describes some non-equilibrium behavior (for example, in the case of our cell division model), but further investigation of more general nonlinear behavior and modulation of wider cell behavior by mtDNA populations (for example, by influencing cell cycle progression[15]) are important future developments. In Supplemental Data Section 1 we discuss a linear stability analysis of our expressions for mean mtDNA behavior, which highlights a link between the "sensing" of an mtDNA species (in the sense that the presence of that species modulates replication or degradation rates) and the ability to control the mean level of that species.

The control of stochastic systems is a well-established field within control theory.[41] Optimal control mechanisms addressing the mean and variance of stochastic processes have been derived in a variety of contexts (see, for example, Borkar[42] and citations therein), particularly in financial applications,[43] and often find tradeoffs between controlling the mean and variance of a process. We observe a comparable tradeoff, that tight control on moments of one species leads to loose control on another. We have focused on providing a general theoretical formalism with which to treat any given control mechanism; it is

anticipated that the above treatment may also be of value in describing heterogeneity in other systems where replication and/or death rates of individuals depend on feedback from current numbers of individuals (for example, through terms describing competition for resources in ecology). Within the context of mtDNA populations, we anticipate that this theoretical framework will assist in understanding natural processes of mtDNA inheritance and evolution within an organismal lifetime (including segregation and increasing variance with age)[14,23] and informing applied approaches to control mitochondrial behavior with genetic tools.[4,5]

Appendix A. Interpretation of Relaxed Replication

The relaxed replication model[1,19] describes a cellular population of mtDNA molecules according to the following algorithm. mtDNAs randomly degrade as a Poisson process with rate $1/\tau$. Every time step Δt, the value of $C(w,m)$, a deterministic function of w and m, is computed, then $\Delta t C(w,m)$ mtDNAs are added to the population. The *genetic* properties of these added mtDNAs are random—each is assigned a genetic type based on a random sampling of the existing populations—but their *physical* properties (i.e., the total copy number added at each step) are deterministic. We argue that, as both replication and degradation of mtDNAs depend on complicated behavior and thermal, microscopic interactions, it makes more sense to model both processes as stochastic. Thus, $C(w,m)$ is interpreted as the rate of a Poisson process describing replication, just as $1/\tau$ is the rate of a Poisson process describing degradation. This interpretation reconciles the nature of the two processes.

Although this feature is less interesting than the underlying scientific behavior, the original algorithm also raises a (not insurmountable) technical problem with implementation. If a time step $\Delta t < 1/C(w,m)$ is chosen, the algorithm will never add any mtDNA to the system. But, in order to suitably characterize the stochastic degradation without using the Gillespie algorithm,[44] it is desirable to choose a time step Δt as low as possible. There is therefore a risk that one or other of the deterministic replication and stochastic degradation processes is inadequately captured in a given simulation protocol.

We have illustrated the excellent agreement between our theoretical approaches and stochastic simulation (for example, Figure 1). To quantitatively connect with previous analyses of specific control strategies, we confirm that the behavior for model A (relaxed replication) matches that observed in previous simulation studies[19] with a back-of-the-envelope calculation.[39] The rate of variance increase with time with $\tau = 5$ days (comparable in magnitude to the $(1-10)\times$ log 2 days used in Chinnery and Samuels[19]) and $w_{opt} = 1{,}000$ from Figure 1 is roughly 40 day^{-1}. Considering 50 years of evolution of this system, we expect a standard deviation of roughly $\sqrt{40\times 50\times 365} \simeq 850$ in mutant copy number. This value is consistent with the simulations in Chinnery and Samuels.[19]

We connect to an additional numerical result in Capps et al.[1] In the absence of a mutant population, the variance of the wild-type population was reported to be stable at $w_{opt}/(2\alpha)$, with the original model interpretation of mtDNA replication as deterministic. Under the interpretation of stochastic replication, an absent mutant population ($m_{ss} = 0$) permits stability in the wild-type population variance, which after a little algebra is calculated to be w_{opt}/α. Intuitively, modeling both replication and degradation as stochastic does not affect mean copy number but does increase variance.

Appendix B. Interpretation of Wright Formula for mtDNA

The Wright formula

$$\langle h^2 \rangle = \langle h \rangle (1 - \langle h \rangle)\left(1 - \left(1 - (2n_e)^{-1}\right)^g\right) \quad \text{(Equation 17)}$$

has been proposed as a model for the time evolution of heteroplasmy variance $\langle h^2 \rangle$ in a population with effective size n_e subject to random partitioning at each of g generations. This picture has been successfully employed to investigate heteroplasmy distributions in real systems,[22] with n_e and g interpreted as parameters of the theory without immediate biological interpretation.

The mapping of the original genetic system considered by Wright[21] to cellular populations of mtDNA requires some discussion. If "generations" are interpreted as cell divisions, the mechanism by which mtDNA copy number is redoubled between divisions is assumed by the model to be deterministic. Cell divisions will result in a halving of the mtDNA population. Application of the Wright model assumes that the original population is thenceforth recovered with no increased variance in the population. In other words, the mtDNA population is assumed to exactly double between divisions with no stochasticity in the process. As we underline in the main text, the effects of (inevitable) stochasticity due to mtDNA turnover are not explicitly captured by the Wright formula. Other complications exist, as described in Wonnapinij et al.,[22] but play less important roles here. As a result, the "bottleneck size" n_e cannot immediately be interpreted as an observable minimum cellular copy number of mtDNA molecules (a quantity that is reported by, for example, a qPCR experiment measuring cellular mtDNA content), but rather the size of an effective "founder" population.

Supplemental Data

Supplemental Data include mathematical derivations, two figures, and two tables and can be found with this article online at http://dx.doi.org/10.1016/j.ajhg.2016.09.016.

Received: April 18, 2016
Accepted: September 22, 2016
Published: October 27, 2016

References

1. Capps, G.J., Samuels, D.C., and Chinnery, P.F. (2003). A model of the nuclear control of mitochondrial DNA replication. J. Theor. Biol. *221*, 565–583.
2. St John, J. (2014). The control of mtDNA replication during differentiation and development. Biochim. Biophys. Acta *1840*, 1345–1354.
3. Wallace, D.C., and Chalkia, D. (2013). Mitochondrial DNA genetics and the heteroplasmy conundrum in evolution and disease. Cold Spring Harb. Perspect. Biol. *5*, a021220.
4. Bacman, S.R., Williams, S.L., Pinto, M., Peralta, S., and Moraes, C.T. (2013). Specific elimination of mutant mitochondrial genomes in patient-derived cells by mitoTALENs. Nat. Med. *19*, 1111–1113.
5. Gammage, P.A., Rorbach, J., Vincent, A.I., Rebar, E.J., and Minczuk, M. (2014). Mitochondrially targeted ZFNs for selective degradation of pathogenic mitochondrial genomes bearing large-scale deletions or point mutations. EMBO Mol. Med. *6*, 458–466.
6. Burgstaller, J.P., Johnston, I.G., and Poulton, J. (2015). Mitochondrial DNA disease and developmental implications for reproductive strategies. Mol. Hum. Reprod. *21*, 11–22.
7. Rossignol, R., Faustin, B., Rocher, C., Malgat, M., Mazat, J.P., and Letellier, T. (2003). Mitochondrial threshold effects. Biochem. J. *370*, 751–762.
8. Baris, O.R., Ederer, S., Neuhaus, J.F., von Kleist-Retzow, J.C., Wunderlich, C.M., Pal, M., Wunderlich, F.T., Peeva, V., Zsurka, G., Kunz, W.S., et al. (2015). Mosaic deficiency in mitochondrial oxidative metabolism promotes cardiac arrhythmia during aging. Cell Metab. *21*, 667–677.
9. Raj, A., and van Oudenaarden, A. (2008). Nature, nurture, or chance: stochastic gene expression and its consequences. Cell *135*, 216–226.
10. Kaern, M., Elston, T.C., Blake, W.J., and Collins, J.J. (2005). Stochasticity in gene expression: from theories to phenotypes. Nat. Rev. Genet. *6*, 451–464.
11. Paulsson, J. (2004). Summing up the noise in gene networks. Nature *427*, 415–418.
12. Lygeros, J., Koutroumpas, K., Dimopoulos, S., Legouras, I., Kouretas, P., Heichinger, C., Nurse, P., and Lygerou, Z. (2008). Stochastic hybrid modeling of DNA replication across a complete genome. Proc. Natl. Acad. Sci. USA *105*, 12295–12300.
13. Kopsidas, G., Kovalenko, S.A., Heffernan, D.R., Yarovaya, N., Kramarova, L., Stojanovski, D., Borg, J., Islam, M.M., Caragounis, A., and Linnane, A.W. (2000). Tissue mitochondrial DNA changes. A stochastic system. Ann. N Y Acad. Sci. *908*, 226–243.
14. Johnston, I.G., Burgstaller, J.P., Havlicek, V., Kolbe, T., Rülicke, T., Brem, G., Poulton, J., and Jones, N.S. (2015). Stochastic modelling, Bayesian inference, and new in vivo measurements elucidate the debated mtDNA bottleneck mechanism. eLife *4*, e07464.
15. Johnston, I.G., Gaal, B., Neves, R.P., Enver, T., Iborra, F.J., and Jones, N.S. (2012). Mitochondrial variability as a source of extrinsic cellular noise. PLoS Comput. Biol. *8*, e1002416.
16. Jajoo, R., Jung, Y., Huh, D., Viana, M.P., Rafelski, S.M., Springer, M., and Paulsson, J. (2016). Accurate concentration control of mitochondria and nucleoids. Science *351*, 169–172.
17. Figge, M.T., Reichert, A.S., Meyer-Hermann, M., and Osiewacz, H.D. (2012). Deceleration of fusion-fission cycles improves mitochondrial quality control during aging. PLoS Comput. Biol. *8*, e1002576.
18. Poovathingal, S.K., Gruber, J., Halliwell, B., and Gunawan, R. (2009). Stochastic drift in mitochondrial DNA point mutations: a novel perspective ex silico. PLoS Comput. Biol. *5*, e1000572.
19. Chinnery, P.F., and Samuels, D.C. (1999). Relaxed replication of mtDNA: A model with implications for the expression of disease. Am. J. Hum. Genet. *64*, 1158–1165.
20. Johnston, I.G., and Jones, N.S. (2015). Closed-form stochastic solutions for non-equilibrium dynamics and inheritance of cellular components over many cell divisions. Proc. Math. Phys. Eng. Sci. *471*, 20150050.
21. Wright, S. (1942). Statistical genetics and evolution. Bull. Am. Math. Soc. *48*, 223–246.
22. Wonnapinij, P., Chinnery, P.F., and Samuels, D.C. (2008). The distribution of mitochondrial DNA heteroplasmy due to random genetic drift. Am. J. Hum. Genet. *83*, 582–593.
23. Burgstaller, J.P., Johnston, I.G., Jones, N.S., Albrechtová, J., Kolbe, T., Vogl, C., Futschik, A., Mayrhofer, C., Klein, D., Sabitzer, S., et al. (2014). MtDNA segregation in heteroplasmic tissues is common in vivo and modulated by haplotype differences and developmental stage. Cell Rep. *7*, 2031–2041.
24. Van Kampen, N. (1992). Stochastic Processes in Physics and Chemistry (Elsevier).
25. Elf, J., and Ehrenberg, M. (2003). Fast evaluation of fluctuations in biochemical networks with the linear noise approximation. Genome Res. *13*, 2475–2484.
26. Assaf, M., and Meerson, B. (2010). Extinction of metastable stochastic populations. Phys. Rev. E Stat. Nonlin. Soft Matter Phys. *81*, 021116.
27. Solignac, M., Génermont, J., Monnerot, M., and Mounolou, J.C. (1987). *Drosophila* mitochondrial genetics: evolution of heteroplasmy through germ line cell divisions. Genetics *117*, 687–696.
28. Wai, T., Teoli, D., and Shoubridge, E.A. (2008). The mitochondrial DNA genetic bottleneck results from replication of a subpopulation of genomes. Nat. Genet. *40*, 1484–1488.
29. Wonnapinij, P., Chinnery, P.F., and Samuels, D.C. (2010). Previous estimates of mitochondrial DNA mutation level variance did not account for sampling error: comparing the mtDNA genetic bottleneck in mice and humans. Am. J. Hum. Genet. *86*, 540–550.
30. Kimura, M. (1955). Solution of a process of random genetic drift with a continuous model. Proc. Natl. Acad. Sci. USA *41*, 144–150.
31. Birky, C.W., Jr. (2001). The inheritance of genes in mitochondria and chloroplasts: laws, mechanisms, and models. Annu. Rev. Genet. *35*, 125–148.
32. Monnot, S., Gigarel, N., Samuels, D.C., Burlet, P., Hesters, L., Frydman, N., Frydman, R., Kerbrat, V., Funalot, B., Martinovic, J., et al. (2011). Segregation of mtDNA throughout human embryofetal development: m.3243A>G as a model system. Hum. Mutat. *32*, 116–125.
33. Lawson, K.A., and Hage, W.J. (1994). Clonal analysis of the origin of primordial germ cells in the mouse. Ciba Found. Symp. *182*, 68–84, discussion 84–91.
34. Cree, L.M., Samuels, D.C., de Sousa Lopes, S.C., Rajasimha, H.K., Wonnapinij, P., Mann, J.R., Dahl, H.H., and Chinnery,

P.F. (2008). A reduction of mitochondrial DNA molecules during embryogenesis explains the rapid segregation of genotypes. Nat. Genet. *40*, 249–254.
35. Cao, L., Shitara, H., Horii, T., Nagao, Y., Imai, H., Abe, K., Hara, T., Hayashi, J., and Yonekawa, H. (2007). The mitochondrial bottleneck occurs without reduction of mtDNA content in female mouse germ cells. Nat. Genet. *39*, 386–390.
36. Jenuth, J.P., Peterson, A.C., Fu, K., and Shoubridge, E.A. (1996). Random genetic drift in the female germline explains the rapid segregation of mammalian mitochondrial DNA. Nat. Genet. *14*, 146–151.
37. Diot, A., Hinks-Roberts, A., Lodge, T., Liao, C., Dombi, E., Morten, K., Brady, S., Fratter, C., Carver, J., Muir, R., et al. (2015). A novel quantitative assay of mitophagy: Combining high content fluorescence microscopy and mitochondrial DNA load to quantify mitophagy and identify novel pharmacological tools against pathogenic heteroplasmic mtDNA. Pharmacol. Res. *100*, 24–35.
38. Pyle, A., Taylor, R.W., Durham, S.E., Deschauer, M., Schaefer, A.M., Samuels, D.C., and Chinnery, P.F. (2007). Depletion of mitochondrial DNA in leucocytes harbouring the 3243A->G mtDNA mutation. J. Med. Genet. *44*, 69–74.
39. Johnston, I.G., Rickett, B.C., and Jones, N.S. (2014). Explicit tracking of uncertainty increases the power of quantitative rule-of-thumb reasoning in cell biology. Biophys. J. *107*, 2612–2617.
40. Johnston, I.G. (2014). Efficient parametric inference for stochastic biological systems with measured variability. Stat. Appl. Genet. Mol. Biol. *13*, 379–390.
41. Åström, K. (2012). Introduction to Stochastic Control Theory (Dover).
42. Borkar, V. (2005). Controlled diffusion processes. Probability Surveys *2*, 213–244.
43. Markowitz, H. (1952). Portfolio selection. J. Finance *7*, 77–91.
44. Gillespie, D. (1977). Exact stochastic simulation of coupled chemical reactions. J. Phys. Chem. *81*, 2340–2361.

The American Journal of Human Genetics, Volume *99*

Supplemental Data

Evolution of Cell-to-Cell Variability in Stochastic, Controlled, Heteroplasmic mtDNA Populations

Iain G. Johnston and Nick S. Jones

Supplementary Information

S1. Expansion of the control law.

If we write $\epsilon_w = w - w_{ss}, \epsilon_m = m - m_{ss}$, the expansion of replication and degradation rates $\lambda(w,m)$ and $\nu(w,m)$ about the steady state $\{w_{ss}, m_{ss}\}$ gives

$$\lambda(w,m) \simeq \lambda(w_{ss},m_{ss}) + \left.\frac{\partial\lambda(w,m)}{\partial w}\right|_{(w_{ss},m_{ss})}\epsilon_w + \left.\frac{\partial\lambda(w,m)}{\partial m}\right|_{(w_{ss},m_{ss})}\epsilon_m + O(\epsilon^2) \quad (1)$$

$$\nu(w,m) \simeq \nu(w_{ss},m_{ss}) + \left.\frac{\partial\nu(w,m)}{\partial w}\right|_{(w_{ss},m_{ss})}\epsilon_w + \left.\frac{\partial\nu(w,m)}{\partial m}\right|_{(w_{ss},m_{ss})}\epsilon_m + O(\epsilon^2). \quad (2)$$

This expansion represents a model of a given control strategy $\lambda(w,m), \nu(w,m)$, which, if the original function is well behaved, we expect to reasonably reflect behaviour of the system close to $\{w_{ss}, m_{ss}\}$. Simulation results show that this expectation is fulfilled for a wide variety of cases (see figures in the Main Text).

To find w_{ss} and m_{ss} we solve the equations describing the deterministic behaviour of the system:

$$\left.\frac{dw}{dt}\right|_{(w_{ss},m_{ss})} = w_{ss}\lambda(w_{ss},m_{ss}) - w_{ss}\nu(w_{ss},m_{ss}) = 0 \quad (3)$$

$$\left.\frac{dm}{dt}\right|_{(w_{ss},m_{ss})} = m_{ss}\lambda(w_{ss},m_{ss}) - m_{ss}\nu(w_{ss},m_{ss}) = 0 \quad (4)$$

It will be observed that for this steady state to exist, the terms $\lambda(w_{ss},m_{ss})$ and $\nu(w_{ss},m_{ss})$ in Eqns. 1-2 must be equal. We can write the general expansion form of $\lambda(w,m)$ and $\nu(w,m)$, truncated to first order, as

$$\lambda(w,m) \simeq \beta_0 + \beta_w(w - w_{ss}) + \beta_m(m - m_{ss}), \quad (5)$$

$$\nu(w,m) \simeq \delta_0 + \delta_w(w - w_{ss}) + \delta_m(m - m_{ss}), \quad (6)$$

with $\beta_w = \partial\lambda/\partial w|_{w_{ss},m_{ss}}, \beta_m = \partial\lambda/\partial m|_{w_{ss},m_{ss}}, \delta_w = \partial\nu/\partial w|_{w_{ss},m_{ss}}, \delta_m = \partial\nu/\partial m|_{w_{ss},m_{ss}}$. Clearly, to support convergence to a steady state, β_w and β_w must be negative and δ_w and δ_m must be positive. Given this model for control dynamics, we next characterise the variance of the system. We can thus describe the system with a set of $R = 4$ processes with rates

$$f_1 = w\left(\beta_0 + \beta_w(w - w_{ss}) + \beta_m(m - m_{ss})\right) \quad (7)$$

$$f_2 = m\left(\beta_0 + \beta_w(w - w_{ss}) + \beta_m(m - m_{ss})\right) \quad (8)$$

$$f_3 = w\left(\delta_0 + \delta_w(w - w_{ss}) + \delta_m(m - m_{ss})\right) \quad (9)$$

$$f_4 = m\left(\delta_0 + \delta_w(w - w_{ss}) + \delta_m(m - m_{ss})\right) \quad (10)$$

and stoichiometry matrix describing the effects of these reactions on the $N = 2$ species we consider as

$$S = ((1,0),(0,1),(-1,0),(0,-1))^T. \quad (11)$$

Using index $i = 1$ to correspond to species w and $i = 2$ to correspond to species m, the master equation for the system, describing the time evolution of $P_{w,m}$ (the probability of observing w wildtype and m mutant mtDNAs) can then be written

$$\frac{\partial P_{w,m}}{\partial t} = \sum_{j=1}^{R}\left(\prod_{i=1}^{N}\mathbb{E}^{-S_{ij}} - 1\right) f_j(w,m)P_{w,m} \quad (12)$$

where $\mathbb{E}^{-S_{ij}}$ takes its normal meaning as a raising and lowering operator [1], adding $-S_{ij}$ to each occurrence of index i that follows it on the right (so e.g. as $S_{11} = 1$ and w corresponds to index 1, $\mathbb{E}^{-S_{11}} f_j(w,m)P_{w,m} \to f_j(w-1,m)P_{w-1,m}$).

The potential nonlinearities and coupling between species in this equation prevents a full general solution. To make progress, we employ Van Kampen's system size expansion [1, 2] and write $w = \phi_w\Omega + \xi_w\Omega^{1/2}, m =$

$\phi_m\Omega + \xi_m\Omega^{1/2}$, representing copy numbers as the sum of deterministic components ϕ_i and fluctuation components ξ_i scaled by powers of system size Ω. Following the standard expansion procedure, by writing $\mathbb{E}$, $P_{w,m}$ and f_i in terms of Ω and collecting powers of Ω in Eqn. 12, first gives equations for the deterministic components of the system (corresponding straightforwardly to the macroscopic rate equations):

$$\frac{\partial \phi_i}{\partial t} = \sum_{j=1}^{R} S_{ij} f_j, \tag{13}$$

then gives a Fokker-Planck equation for the time behaviour of the fluctuation components in terms of the bivariate probability distribution $\Pi(\xi, t)$ of $\xi = (\xi_w, \xi_m)$ at time t:

$$\frac{\partial \Pi(\xi,t)}{\partial t} = \sum_{i,j=1}^{N} A_{ij} \frac{\partial(\xi_j \Pi)}{\partial \xi_i} + \frac{1}{2} \sum_{i,j=1}^{N} B_{ij} \frac{\partial^2 \Pi}{\partial \xi_i \, \partial \xi_j}, \tag{14}$$

where

$$A_{ij} = \sum_{k=1}^{R} S_{ik} \frac{\partial f_k}{\partial \phi_j}, \tag{15}$$

$$B_{ij} = \sum_{k=1}^{R} S_{ik} S_{jk} f_k. \tag{16}$$

The form of Eqns. 7-10 and Eqn. 11 gives, for steady state copy numbers and $\delta_0 = \beta_0$, $A_{11} = \kappa_w w_{ss}, A_{12} = \kappa_m w_{ss}, A_{21} = \kappa_w m_{ss}, A_{22} = \kappa_m m_{ss}, B_{11} = 2\beta_0 w_{ss}, B_{22} = 2\beta_0 m_{ss}, B_{12} = B_{21} = 0$, where $\kappa_w = (\beta_w - \delta_w), \kappa_m = (\beta_m - \delta_m)$. From this Fokker-Planck equation expressions for the moments of ξ_i can be extracted [1], leading to the expressions:

$$\frac{d\langle \xi_w^2 \rangle}{dt} = 2A_{11}\langle \xi_w^2 \rangle + 2A_{12}\langle \xi_w \xi_m \rangle + B_{11} \tag{17}$$

$$\frac{d\langle \xi_w \xi_m \rangle}{dt} = (A_{11} + A_{22})\langle \xi_w \xi_m \rangle + A_{12}\langle \xi_m^2 \rangle + A_{21}\langle \xi_w^2 \rangle + B_{12} \tag{18}$$

$$\frac{d\langle \xi_m^2 \rangle}{dt} = 2A_{22}\langle \xi_m^2 \rangle + 2A_{21}\langle \xi_w \xi_m \rangle + B_{22}, \tag{19}$$

A linear stability analysis of the deterministic ODEs describing mean behaviour is straightforward to perform. Linearising Eqns. 3-4 about (w_{ss}, m_{ss}) gives

$$\frac{dw}{dt} \simeq (\beta_w - \delta_w) w_{ss}(w - w_{ss}) + O(w^2) + O(wm) \tag{20}$$

$$\frac{dm}{dt} \simeq (\beta_m - \delta_m) m_{ss}(m - m_{ss}) + O(m^2) + O(wm), \tag{21}$$

from which it is straightforward to see that if $\kappa_w < 0$ and $\kappa_m < 0$, the mean dynamics of w and m respectively are linearly stable. This condition is met for w and m in control laws A and E, for w in B, C, and F, and for neither in D. These specific examples illustrate the principle that if a species is explicitly 'sensed' – in the sense that it modulates replication or degradation rate – its mean dynamics can be controlled to be linearly stable. If a species is not explicitly sensed (replication and degradation are not functions of its copy number) then its mean dynamics are not explicitly linearly stable, but may be 'balanced', as the corresponding κ term is zero. Perturbations in these unsensed 'balanced' variables are neither damped away by control nor guaranteed to explode with time; hence the variables are unconstrained but not explicitly unstable.

S2. Full solutions for steady state ODEs.

Eqns. 17-19 can be solved exactly for the A_{ij}, B_{ij} corresponding to the steady state condition above. The complete solutions for arbitrary $\langle \xi_w^2 \rangle, \langle \xi_w \xi_m \rangle, \langle \xi_m^2 \rangle$ at $t = 0$ are lengthy and do not allow much intuitive interpretation. For $\langle \xi_w^2 \rangle = \langle \xi_w \xi_m \rangle = \langle \xi_m^2 \rangle = 0$ at $t = 0$ (noiseless initial conditions), we can solve and separate the long-term

behaviour from the transient behaviour. The transients, given by Eqns. 25-27 below, involve terms in $t' \equiv \exp((\kappa_m m_{ss} + \kappa_w w_{ss})t)$. As the κ_i are nonpositive (for stability, β_i are nonpositive and δ_i are nonnegative), t' is either a constant or an exponentially decaying function of time t; in the cases we consider, it either decays with time (all models except D) or the associated term is always zero (model D).

$$\begin{aligned}
\langle \xi_w^2 \rangle &= F_1^{decay}(t') + \left(\frac{2\beta_0 m_{ss} w_{ss}(m_{ss} + w_{ss})\kappa_m^2}{(m_{ss}\kappa_m + w_{ss}\kappa_w)^2} \right) t \\
&\quad + \left(\frac{-\beta_0 w_{ss}^2(w_{ss}\kappa_w^2 + m_{ss}\kappa_m(4\kappa_w - 3\kappa_m))}{(m_{ss}\kappa_m + w_{ss}\kappa_w)^3} \right) \qquad (22) \\
\langle \xi_w \xi_m \rangle &= F_2^{decay}(t') + \left(\frac{-2\beta_0 m_{ss} w_{ss}(m_{ss} + w_{ss})\kappa_m \kappa_w}{(m_{ss}\kappa_m + w_{ss}\kappa_w)^2} \right) t \\
&\quad + \left(\frac{\beta_0 m_{ss} w_{ss}(m_{ss}\kappa_m(\kappa_m - 2\kappa_w) + w_{ss}\kappa_w(\kappa_w - 2\kappa_m))}{(m_{ss}\kappa_m + w_{ss}\kappa_w)^3} \right) \qquad (23) \\
\langle \xi_m^2 \rangle &= F_3^{decay}(t') + \left(\frac{2\beta_0 m_{ss} w_{ss}(m_{ss} + w_{ss})\kappa_w^2}{(m_{ss}\kappa_m + w_{ss}\kappa_w)^2} \right) t \\
&\quad + \left(\frac{-\beta_0 m_{ss}^2(m_{ss}\kappa_m^2 + w_{ss}\kappa_w(4\kappa_m - 3\kappa_w))}{(m_{ss}\kappa_m + w_{ss}\kappa_w)^3} \right), \qquad (24)
\end{aligned}$$

where the F_i^{decay} functions characterising the transient behaviour are

$$\begin{aligned}
F_1^{decay}(t') &= \frac{\beta_0 w_{ss}^2 t'(\kappa_w^2 w_{ss} t' + \kappa_m m_{ss}(\kappa_m(t' - 4) + 4\kappa_w))}{(\kappa_m m_{ss} + \kappa_w w_{ss})^3} \qquad (25) \\
F_2^{decay}(t') &= \frac{\beta_0 w_{ss} m_{ss} t'(\kappa_m^2 m_{ss}(t' - 2) + 2(m_{ss} + w_{ss})\kappa_w \kappa_m + \kappa_w^2 w_{ss}(t' - 2))}{(\kappa_m m_{ss} + \kappa_w w_{ss}^2)^3}, \qquad (26) \\
F_3^{decay}(t') &= \frac{\beta_0 m_{ss}^2 t'(\kappa_m^2 m_{ss} t' + \kappa_w w_{ss}(\kappa_w(t' - 4) + 4\kappa_m))}{(\kappa_m m_{ss} + \kappa_w w_{ss})^3} \qquad (27) \\
&\qquad (28)
\end{aligned}$$

Eqns. 22-24 with Eqns. 25-27 then give the full transient behaviour displayed in Fig. 1 in the Main Text , decaying to the aforementioned linear behaviour with characteristic timescale $(\kappa_m m_{ss} + \kappa_w w_{ss})$.

S3. Interpretation and behaviour of specific control strategies.

The mechanisms described in the Main Text have simple interpretations in the language of stochastic processes. Mechanism A, as discussed, corresponds to the 'relaxed replication' picture studied previously (Appendix A1). Mechanism D corresponds to independent birth-death processes acting on both species (analysed in [3]). Mechanism F corresponds to an immigration-death process acting on the wildtype (the dependence of replication rate on $1/w$ means that overall production is constant with time), and model C can be regarded as a birth-immigration-death process on the wildtype (analysed in [4]). Both these mechanisms are thus expected to tightly control wildtype behaviour (including controlling variance: immigration-death processes yield a constant steady-state variance), but do not sense (and, therefore, do not apply feedback to) mutant load. We also note that mechanisms F and G are in a sense 'dual', in that they apply similar control manifest through replication with rate $\sim 1/w$ and degradation with rate w respectively. The previous result that control applied to (a) biogenesis rates and (b) degradation rates yields similar population behaviour is visible in the behaviour of F and G in Fig. 1 in the Main Text .

Table S1 gives, for each example control strategy in the Main Text, the corresponding steady state $\{w_{ss}, m_{ss}\}$ and the expansion terms for the strategy β, δ. The corresponding behaviours of variances, from Eqns. 22-24, are given in Table S2 .

In the Main Text we discuss the implications of an increasing extinction probability of one mtDNA type. A non-negligible extinction probability challenges the validity of the linear noise approximation and leads to departure from results derived using the system size expansion. To illustrate this behaviour, we reduce the characteristic timescale of the parameterisations used to explore models A-G in the Main Text, setting $\tau = 1$ rather than $\tau = 5$, and simulate for a longer time window (see Fig. S1). It will be observed that as extinction probability increases (as $\sqrt{\langle m^2 \rangle} \to \langle m \rangle$), the numerical behaviour departs from that predicted analytically; in particular, the increase of $\langle h^2 \rangle$ slows from a linear to sublinear regime as discussed in the Main Text.

We note that, in some physiological circumstances, the representation of one mtDNA type in a cellular population may be low – for example, the appearance of one mutant mtDNA through *de novo* mutation or replication error, or the presence of a small percentage of a foreign mtDNA haplotype due to carryover in gene therapies [5]. In these cases, a non-negligible extinction probability may occur quickly and the transition of $\langle h^2 \rangle$ to a sublinear, or flat, regime will be an important aspect of the long-term dynamics. In the case of mtDNA disease inheritance, however, situations with a macroscopic fraction of mutant mtDNA are often the most important, due to the presence of a 'heteroplasmy threshold' [6] beyond which disease symptoms manifest. With two mtDNA haplotypes represented in comparable proportions in the cell, our linear analysis holds and can be used to describe heteroplasmy variance in somatic and germline cells.

S4. Steady state solution.

Eqns. 17-19 give, for steady state,

$$\begin{aligned} 2w_{ss}(\beta_0 + \kappa_m \langle \xi_w \xi_m \rangle + \kappa_w \langle \xi_w^2 \rangle) &= 0 \quad (29) \\ w_{ss}\kappa_m \langle \xi_m^2 \rangle + m_{ss}\kappa_w \langle \xi_w^2 \rangle + (m_{ss}\kappa_m + w_{ss}\kappa_w)\langle \xi_w \xi_m \rangle &= 0 \quad (30) \\ 2m_{ss}(\beta_0 + \kappa_m \langle \xi_m^2 \rangle + \kappa_w \langle \xi_w \xi_m \rangle) &= 0 \quad (31) \end{aligned}$$

Attempting to solve these equations for $\langle \xi_w^2 \rangle$, then $\langle \xi_w \xi_m \rangle$, then $\langle \xi_m^2 \rangle$ first gives $\langle \xi_w^2 \rangle = (-\beta_0 - \kappa_m \langle \xi_w \xi_m \rangle)/\kappa_w$, then $\langle \xi_w \xi_m \rangle = (\beta_0 m_{ss} - \kappa_m w_{ss} \langle \xi_m^2 \rangle)/(w_{ss}\kappa_w)$, leaving Eqn. 30 reduced to

$$\frac{2\beta_0 m_{ss}(m_{ss} + w_{ss})}{w_{ss}} = 0, \quad (32)$$

a condition only fulfilled (due to the non-negativity of m_{ss} and w_{ss}) if $m_{ss} = 0$. If one proceeds through the analysis by first solving for $\langle \xi_m^2 \rangle$, then $\langle \xi_w \xi_m \rangle$, then $\langle \xi_w^2 \rangle$, a symmetric expression is obtained

$$\frac{2\beta_0 w_{ss}(m_{ss} + w_{ss})}{m_{ss}} = 0. \quad (33)$$

Eqns. 32-33 illustrate the symmetry in the system: if the copy number of either species is zero then a situation where variance does not increase is supported (but not inevitable: compare the behaviour of relaxed replication model (A, fixed variance) and the birth-death model (D, increasing variance) in the case of zero mutant population).

The effect of selection, mutations, and replicative errors on mtDNA variances can straightforwardly be included in this analysis. In this general case, we replace Eqns. 1-4 in the Main Text with:

$$\begin{aligned} \{w, m\} &\xrightarrow{\epsilon_1 + (1+\epsilon_2) w \lambda(w,m)} \{w+1, m\} \quad (34) \\ \{w, m\} &\xrightarrow{\epsilon_3 + (1+\epsilon_4) m \lambda(w,m)} \{w, m+1\} \quad (35) \\ \{w, m\} &\xrightarrow{\epsilon_5 + (1+\epsilon_6) w \nu(w,m)} \{w-1, m\} \quad (36) \\ \{w, m\} &\xrightarrow{\epsilon_7 + (1+\epsilon_8) m \nu(w,m)} \{w, m-1\} \quad (37) \\ \{w, m\} &\xrightarrow{w\mu_1} \{w-1, m+1\} \quad (38) \\ \{w, m\} &\xrightarrow{w\mu_2} \{w, m+1\} \quad (39) \\ \{w, m\} &\xrightarrow{w\mu_3} \{w-1, m+2\}. \quad (40) \end{aligned}$$

Here, we have added processes corresponding to spontaneous mutation of a given wildtype mtDNA (μ_1), and two types of replicative error affecting wildtype mtDNA, giving rise to one (μ_2; original molecule remains intact, new molecule is mutated) and two (μ_3; both original and new molecules are mutated) mutant mtDNAs respectively. Differences manifest either through replicative or degradation advantages (or both) are incorporated with even-indexed ϵ_i (providing multiplicative changes to the bare rates) and odd-indexed ϵ_i (providing additive changes). We thus have two ways of provoking selective advantages in each case: increasing wildtype biogenesis, increasing mutant biogenesis, increasing wildtype degradation, and increasing mutant degradation.

Fig. S2 shows example trajectories arising from each of our control mechanisms in the presence of the mutation processes above, and the selective pressures $(\epsilon_3, \epsilon_4, \epsilon_5, \epsilon_6)$ that favour mutant mtDNA. An excellent agreement between ODE theory and stochastic simulation is again illustrated, and there is substantial similarity between

the behaviours caused by selection (favouring mutant mtDNA) and mutation (producing mutant mtDNA). In several cases (mechanisms B, C, F, G), $\langle m \rangle$ and $\langle m^2 \rangle$ simply increase exponentially with time under favourable selective or mutational pressures; this situation straightforwardly gives rise to a sigmoidal change in heteroplasmy $\langle h \rangle \sim 1/(1 + e^{-\Delta f t}(1 - h_0)/h_0)$, with Δf an effective selective difference, as used in previous work [7, 8]. In mechanisms coupling wildtype and mutant content (A and E), mutant increase is slower and accompanied by a decrease in wildtype, attempting to keep total copy number constant. In these circumstances, variance behaviour can be more complex: for example, under relaxed replication with pressure favouring mutant mtDNA, $\langle w^2 \rangle$ initially increases then subsequently decreases as $\langle w \rangle$ decreases in magnitude. Mechanism D, where control does not couple mutant and wildtype, has correspondingly perpendicular trajectories in $(\langle w \rangle, \langle m \rangle)$ space under different selective pressures, but the coupling action of the mutation operations lead to curved trajectories under mutational influence.

S5. Heteroplasmy.

For a general function $h = h(x, y)$,

$$\langle h^2 \rangle = \langle (h - \langle h \rangle)^2 \rangle. \tag{41}$$

We will consider an expansion about (x_0, y_0), a state such that $h(x_0, y_0) = \langle h \rangle$. Using the first-order Taylor expansion of $h(x, y)$ around (x_0, y_0):

$$\begin{aligned}
\langle h^2 \rangle &= \langle (h - \langle h \rangle)^2 \rangle & (42)\\
&\simeq \left\langle \left(h(x_0, y_0) + (x - x_0) \left.\frac{\partial h}{\partial x}\right|_{(x_0,y_0)} + (y - y_0) \left.\frac{\partial h}{\partial y}\right|_{(x_0,y_0)} - h(x_0, y_0) \right)^2 \right\rangle & (43)\\
&= \left\langle (x - x_0)^2 \left(\frac{\partial h}{\partial x}\right)^2_{(x_0,y_0)} + (y - y_0)^2 \left(\frac{\partial h}{\partial y}\right)^2_{(x_0,y_0)} + 2(x - x_0)(y - y_0) \left(\frac{\partial h}{\partial x}\frac{\partial h}{\partial y}\right)_{(x_0,y_0)} \right\rangle & (44)\\
&= \langle x^2 \rangle \left(\frac{\partial h}{\partial x}\right)^2_{(x_0,y_0)} + \langle y^2 \rangle \left(\frac{\partial h}{\partial y}\right)^2_{(x_0,y_0)} + 2\langle xy \rangle \left(\frac{\partial h}{\partial x}\frac{\partial h}{\partial y}\right)_{(x_0,y_0)}. & (45)
\end{aligned}$$

We now consider $h(x, y) = x/y$, so that

$$\begin{aligned}
\langle h^2 \rangle &\simeq \left(\langle x^2 \rangle \frac{1}{y^2} + \langle y^2 \rangle \frac{x^2}{y^4} - 2\langle xy \rangle \frac{x}{y^3} \right)_{(x_0,y_0)} & (46)\\
&= \left(\frac{x^2}{y^2} \left(\frac{\langle x^2 \rangle}{x^2} + \frac{\langle y^2 \rangle}{y^2} - \frac{2\langle xy \rangle}{xy} \right) \right)_{(x_0,y_0)}. & (47)
\end{aligned}$$

Finally, given that $x_0 = \langle x \rangle$ and $y_0 = \langle y \rangle$, and setting $x \equiv m$ and $y \equiv w + m$, we obtain

$$\langle h^2 \rangle \simeq \frac{\langle m \rangle^2}{\langle w + m \rangle^2} \left(\frac{\langle m^2 \rangle}{\langle m \rangle^2} + \frac{\langle (w + m)^2 \rangle}{\langle w + m \rangle^2} - \frac{2\langle m(w + m) \rangle}{\langle m \rangle \langle w + m \rangle} \right) \tag{48}$$

To see that exponential growth or decay in one mtDNA type while the other remains constant gives rise to sigmoidal heteroplasmy dynamics, consider (without loss of generality) $m = h_0 n_0 e^{\beta t}, w = (1 - h_0)n_0$, where n_0 is an initial population size which will cancel. Then, as m (and hence $n = m + w$) increases with time,

$$h = \frac{m}{m + w} = \frac{h_0 n_0 e^{\beta t}}{n_0(h_0 e^{\beta t} + (1 - h_0))} = \frac{1}{1 + \frac{1-h_0}{h_0} e^{-\beta t}}, \tag{49}$$

as used in Refs. [5] and [3], with β corresponding to a selective pressure (in this derivation, positive β favours mutant mtDNA).

S6. Fokker-Planck terms for nonequilibrium regimes.

The system size expansion approach above can be applied to the general system without employing an expansion of the control strategy about a steady state, by considering the processes

$$
\begin{aligned}
f_1 &= w\lambda_w(w,m) && (50)\\
f_2 &= m\lambda_m(w,m) && (51)\\
f_3 &= w\nu_w(w,m) && (52)\\
f_4 &= m\nu_m(w,m) && (53)
\end{aligned}
$$

If the expansion about steady state is not used, the corresponding terms are

$$
\begin{aligned}
A_{11} &= \lambda_w(\phi_w,\phi_m) - \nu_w(\phi_w,\phi_m) + \phi_w(\partial_w\lambda_w(\phi_w,\phi_m) - \partial_w\nu_w(\phi_w,\phi_m)) && (54)\\
A_{12} &= \phi_w(\partial_m\lambda_w(\phi_w,\phi_m) - \partial_m\nu_w(\phi_w,\phi_m)) && (55)\\
A_{21} &= \phi_m(\partial_w\lambda_m(\phi_w,\phi_m) - \partial_w\nu_m(\phi_w,\phi_m)) && (56)\\
A_{22} &= \lambda_m(\phi_w,\phi_m) - \nu_m(\phi_w,\phi_m) + \phi_m(\partial_m\lambda_m(\phi_w,\phi_m) - \partial_m\nu_m(\phi_w,\phi_m)) && (57)\\
B_{11} &= \phi_w(\lambda_w(\phi_w,\phi_m) + \nu_w(\phi_w,\phi_m)) && (58)\\
B_{22} &= \phi_m(\lambda_w(\phi_w,\phi_m) + \nu_w(\phi_w,\phi_m)) && (59)\\
B_{12} &= B_{21} = 0, && (60)
\end{aligned}
$$

where $\partial_x f(\phi_i,\phi_j)$ means $\left.\frac{\partial f}{\partial x}\right|_{\phi_i,\phi_j}$. We include the mutational processes in the text by adding $f_5 = \mu_1 w, f_6 = \mu_2 w, f_7 = \mu_3 w$ and setting the corresponding stoichiometry matrix to

$$
S = ((1,0),(0,1),(-1,0),(0,-1),(-1,1),(0,1),(-1,2))^T. \quad (61)
$$

If $\lambda_w = \lambda_m = \lambda$ and $\nu_w = \nu_m = \nu$ (no selective differences between mtDNA types), the Fokker-Planck terms become

$$
\begin{aligned}
A_{11} &= -\mu_1 - \mu_3 + \lambda(\phi_w,\phi_m) - \nu(\phi_w,\phi_m) + \phi_w(\partial_w\lambda(\phi_w,\phi_m) - \partial_w\nu(\phi_w,\phi_m)) && (62)\\
A_{12} &= \phi_w(\partial_m\lambda(\phi_w,\phi_m) - \partial_m\nu(\phi_w,\phi_m)) && (63)\\
A_{21} &= \mu_1 + \mu_2 + 2\mu_3 + \phi_m(\partial_w\lambda(\phi_w,\phi_m) - \partial_w\nu(\phi_w,\phi_m)) && (64)\\
A_{22} &= \lambda(\phi_w,\phi_m) - \nu(\phi_w,\phi_m) + \phi_m(\partial_m\lambda(\phi_w,\phi_m) - \partial_m\nu(\phi_w,\phi_m)) && (65)\\
B_{11} &= \phi_w(\mu_1 + \mu_3 + \lambda(\phi_w,\phi_m) + \nu(\phi_w,\phi_m)) && (66)\\
B_{22} &= (\mu_1 + \mu_2 + 4\mu_3) + \phi_m(\lambda(\phi_w,\phi_m) + \nu(\phi_w,\phi_m)) && (67)\\
B_{12} &= B_{21} = -(\mu_1 + 2\mu_3)\phi_w. && (68)
\end{aligned}
$$

Including selection terms (without mutation) requires no change to the original structure of reactions and stoichiometries and immediately gives

$$
\begin{aligned}
A_{11} &= (1+\epsilon_2)\lambda(\phi_w,\phi_m) - (1+\epsilon_6)\nu(\phi_w,\phi_m) + \phi_w((1+\epsilon_2)\partial_w\lambda(\phi_w,\phi_m) - (1+\epsilon_6)\partial_w\nu(\phi_w,\phi_m)) && (69)\\
A_{12} &= \phi_w((1+\epsilon_2)\partial_m\lambda(\phi_w,\phi_m) - (1+\epsilon_6)\partial_m\nu(\phi_w,\phi_m)) && (70)\\
A_{21} &= \phi_m((1+\epsilon_4)\partial_w\lambda(\phi_w,\phi_m) - (1+\epsilon_8)\partial_w\nu(\phi_w,\phi_m)) && (71)\\
A_{22} &= (1+\epsilon_4)\lambda(\phi_w,\phi_m) - (1+\epsilon_8)\nu(\phi_w,\phi_m) + \phi_m((1+\epsilon_4)\partial_m\lambda(\phi_w,\phi_m) - (1+\epsilon_8)\partial_m\nu(\phi_w,\phi_m)) && (72)\\
B_{11} &= \epsilon_1 + \epsilon_5 + \phi_w((1+\epsilon_2)\lambda(\phi_w,\phi_m) + (1+\epsilon_6)\nu(\phi_w,\phi_m)) && (73)\\
B_{22} &= \epsilon_3 + \epsilon_7 + \phi_m((1+\epsilon_4)\lambda(\phi_w,\phi_m) + (1+\epsilon_8)\nu(\phi_w,\phi_m)) && (74)\\
B_{12} &= B_{21} = 0, && (75)
\end{aligned}
$$

The same approach as above can be used to obtain Eqns. 17-19 for the time evolution of fluctuation moments, this time valid for a full temporal trajectory of the system.

S7. Experimental observations to distinguish mechanisms.

Our theoretical results suggest measurements to further elucidate the control mechanisms underlying mtDNA evolution within cells, without using heteroplasmy variance $\langle h^2 \rangle$ (the shortcomings of which are manifest because

seven different feedback controls all yield the same dynamics in $\langle h^2 \rangle'$ – Fig. 1 in the Main Text), and in conjunction with further molecular elucidation of processes governing mtDNA [9, 10] which providing bounds on the types and rates of molecular processes involved (for example, disallowing unphysically high rates of mtDNA replication).

If $\langle w^2 \rangle$ increases with time, mechanisms with weaker constraints on wildtype copy number are more likely (including relaxed replication (A), mechanisms sensing a combination of mutant and wildtype copy number (E), and the case with no feedback (D)). If $\langle w^2 \rangle$ is low and constant, mechanisms involving differential (B) or ratiometric (C) control are likely. If $\langle w^2 \rangle$ is high and constant (of the order of $\langle w \rangle$), mechanisms resembling immigration-death processes (with propagation scaled by inverse copy number, F and G) are more likely. The behaviour of $\langle wm \rangle$ can be used to further distinguish mechanisms which strongly couple wildtype and mutant (including relaxed replication and total copy number control) from those with less coupling.

In all these cases, the likelihood functions associated with specific biological observations will be complicated. Model selection and inference in this case could be performed through comparison to simulation, or using likelihood-free inference [11] for the mean and variance of mtDNA populations [12].

S8. Back-of-the-envelope calculations for leukocyte heteroplasmy measurements.

Average cellular mtDNA copy number measurements in Ref. [13] are made by normalising the signal from the mtDNA-encoded *ND1* gene by that from the nuclear-encoded *GADPH* genes using real-time PCR using iQ Sybr Green on the BioRad ICycler. The published protocol [14] for this technique suggests using 50ng-5pg of genomic DNA. Diploid human cells contain $\sim$ 6pg of genomic DNA; the mass of several hundred (much smaller) mtDNA genomes is negligible by comparison. The protocol thus implies the presence of 1-10000 cells' genomic DNA content; we assume 1000 as an estimate consistent with qPCR standards (Joerg Burgstaller, personal communication).

In our analysis of the data from Ref. [13] we use $\tau = 5$ days and the processes:

$$\{w, m\} \xrightarrow{w\lambda} \{w+1, m\} \tag{76}$$

$$\{w, m\} \xrightarrow{m\lambda} \{w, m+1\} \tag{77}$$

$$\{w, m\} \xrightarrow{w\nu} \{w-1, m\} \tag{78}$$

$$\{w, m\} \xrightarrow{(1+\epsilon_8)m\nu} \{w, m-1\} \tag{79}$$

with $\lambda = \nu = 1/\tau$, and ϵ_8 a selective difference acting to increase degradation of the mutant mtDNA species. We first estimate a value for ϵ_8 consistent with the heteroplasmy changes involved. Using the transformation

$$\beta t = \log\left(\frac{h(h_0 - 1)}{h_0(h - 1)}\right), \tag{80}$$

from Eqn. 49 above, where h_0 is initial heteroplasmy and h is heteroplasmy at time t, we obtain an estimate $\bar{\beta} = -1.2 \times 10^{-4}$ day^{-1}. We thus set $\epsilon_8 = 1.2 \times 10^{-4}$ day^{-1}, to produce the required selective difference manifest through mutant degradation.

Solving the ODEs arising from our theoretical approach (Eqns. 17-19) then give values for $\langle w^2 \rangle$ and $\langle m^2 \rangle$ over time for a given initial condition. Assuming that each datapoint consists of a sample of 10^3 cells, we divide these values by 10^3 to obtain an estimated distribution for each later w, m pair, given the paired initial w, m state. We combine these distrbutions to build an overall distribution over later results, and use the Kolmogorov-Smirnov test to test the alternative hypothesis that the later results were incompatible with draws from this distribution. The results were $p = 0.054$ for wildtype mtDNA copy number and $p = 0.861$ for mutant mtDNA copy number. As highlighted in the text, the absence of a $p < 0.05$ result cannot be interpreted as support for the null hypothesis, but this analysis suggests that the available data is not incompatible with the predictions of our model.

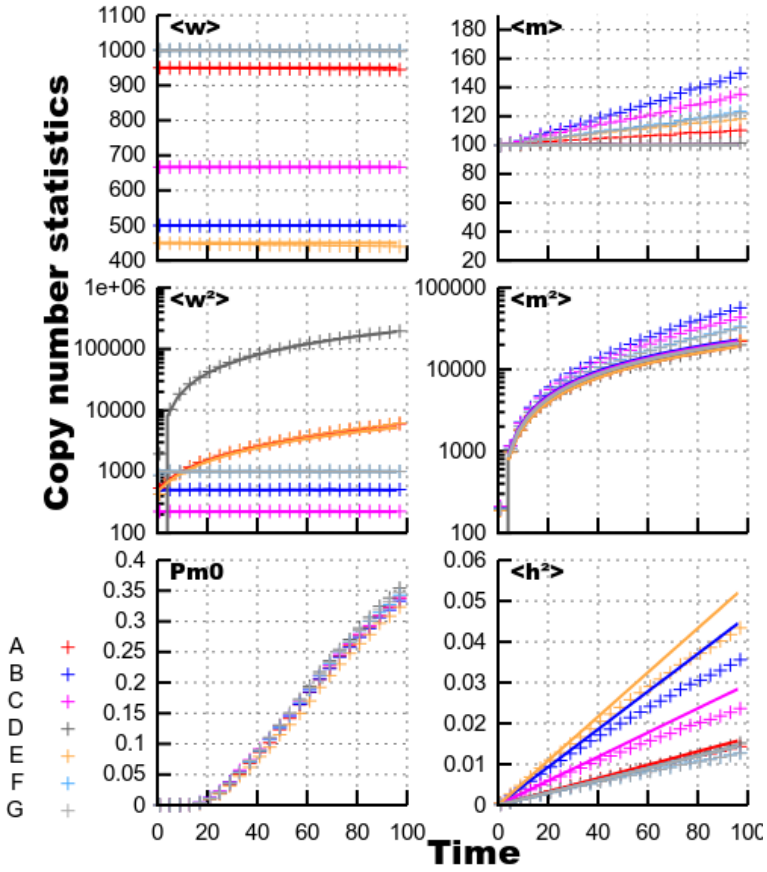

Figure S1: **Influence of fixation on expansion analysis.** The models from the Main Text, simulated for a longer time window and for a shorter characteristic timescale τ, illustrating the behaviour of the systems when extinction becomes possible. $Pm0$ gives the numerically computed probability that $m = 0$; it can be seen that an increase in this quantity corresponds to a moderate increase of $\langle m \rangle$ and $\langle m^2 \rangle$ relative to their predicted values, and a decrease of $\langle h^2 \rangle$ relative to its predicted value (shifting towards a sublinear increase as discussed in the Main Text).

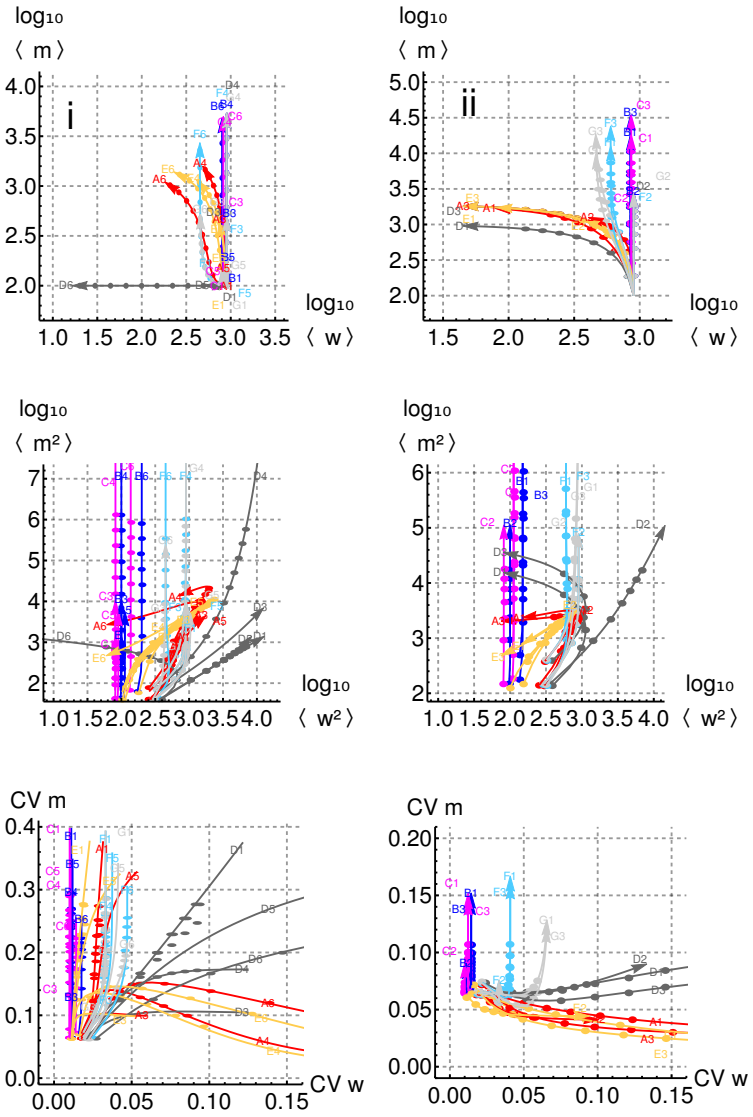

Figure S2: **MtDNA copy number and variability under mutational and selective advantages for mutant mtDNA.** Mean, variance, and CV trajectories with (i) selection pressures, and (ii) mutation rates favouring mutant mtDNA, under models A-G from the text. Some control strategies (A, E) keep mutant relatively bound but sacrifice wildtype and provoke large increases in variability; others (B, C, F, G) focus on wildtype stability, allowing mutant to grow unbound. Labels give the control model (letter) and the parameter varied ($\epsilon_3 = 20; \epsilon_4 = 1; \epsilon_5 = 20; \epsilon_6 = 1$ for (i); $\mu_1 = 0.1; \mu_2 = 0.1; \mu_3 = 0.1$ for (ii)); all other ϵ, μ parameters are set to zero. Results are shown for theory (lines) and stochastic simulation (points), progressing from an initial condition with $w_0 = 900, m_0 = 100$ with the parameterisations in Fig. 1 in the Main Text .

Control	$\lambda(w,m)$ ($\nu(w,m)$ for G)	w_{ss}	m_{ss}	β_w (δ_w for G)	β_m (δ_m for G)
A	$\frac{\alpha(w_{opt}-w-\gamma m)+w+\gamma m}{\tau(w+m)}$	$\frac{w_0 w_{opt}\alpha}{m_0+w_0\alpha+\gamma m_0(\alpha-1)}$	$\frac{m_0 w_{opt}\alpha}{m_0+w_0\alpha+\gamma m_0(\alpha-1)}$	$\frac{-m_0-w_0\alpha-m_0\gamma(\alpha-1)}{m_0 w_{opt}\tau+w_0 w_{opt}\tau}$	$\frac{-(1+(\alpha-1)\gamma)(m_0+w_0\alpha+m_0(\alpha-1)\gamma)}{(m_0+w_0)w_{opt}\alpha\tau}$
B	$\alpha(w_{opt}-w)$	$w_{opt}-1/\alpha\tau$	$\frac{m_0}{w_0}(w_{opt}-1/\alpha\tau)$	$-\alpha$	0
C	$\alpha\left(\frac{w_{opt}}{w}-1\right)$	$\frac{w_{opt}\alpha\tau}{1+\alpha\tau}$	$\frac{m_0}{w_0}\frac{w_{opt}\alpha\tau}{1+\alpha\tau}$	$\frac{-(1+\alpha\tau)^2}{w_{opt}\alpha\tau^2}$	0
D	$1/\tau$	w_0	m_0	0	0
E	$\alpha w_{opt}-\alpha w-\alpha_m m$	$\frac{w_0(w_{opt}\alpha\tau-1)}{\tau(w_0\alpha+m_0\alpha_m)}$	$\frac{m_0(w_{opt}\alpha\tau-1)}{\tau(w_0\alpha+m_0\alpha_m)}$	$-\alpha$	$-\alpha_m$
F	$1/w$	$\alpha\tau$	$\frac{m_0}{w_0}\alpha\tau$	$\frac{-1}{\alpha\tau^2}$	0
G	$1/\tau-\frac{w_{opt}-w}{w_{opt}\tau}$	w_{opt}	$\frac{m_0 w_{opt}}{w_0}$	$\frac{1}{w_{opt}\tau}$	0

Table S1: **Steady states and expansion terms for control strategies A-G.**

Control	Time-independent part of $\langle \xi_w^2 \rangle$	Time-independent part of $\langle \xi_w \xi_m \rangle$	Time-independent part of $\langle \xi_m^2 \rangle$
A	$\frac{w_0^2(m_0+w_0)w_{opt}\alpha(w_0\alpha^2-m_0(1+\gamma(\alpha-1))(3-4\alpha+3\gamma(\alpha-1)))}{(m_0+w_0\alpha+m_0(\alpha-1)\gamma)^4}$	$\frac{-m_0w_0(m_0+w_0)w_{opt}\alpha(m_0(1+\alpha(\gamma-2)-\gamma)(1+\gamma(\alpha-1))+w_0\alpha(\alpha-2+2\gamma-2\alpha\gamma))}{(m_0+w_0\alpha+m_0(\alpha-1)\gamma)^4}$	$\frac{m_0^2(m_0+w_0)w_{opt}\alpha(m_0(1+\gamma(\alpha-1))^2+w_0\alpha(4-3\alpha+4\gamma(\alpha-1)))}{(m_0+w_0\alpha+m_0(\alpha-1)\gamma)^4}$
B	$\frac{1}{\alpha\tau}$	$\frac{-m_0}{w_0\alpha\tau}$	$\frac{-3m_0^2}{w_0^2\alpha\tau}$
C	$\frac{w_{opt}\alpha\tau}{(1+\alpha\tau)^2}$	$\frac{-m_0w_{opt}\alpha\tau}{w_0(1+\alpha\tau)^2}$	$\frac{-3m_0^2w_{opt}\alpha\tau}{(w_0+w_0\alpha\tau)^2}$
D	0	0	0
E	$\frac{w_0^2(w_0\alpha^2+\alpha_m m_0(4\alpha-3\alpha_m)}{(\alpha w_0+\alpha_m m_0)^3\tau}$	$\frac{m_0w_0(2\alpha\alpha_m(m_0+w_0)-w_0\alpha^2-m_0\alpha_m^2)}{(\alpha w_0+\alpha_m m_0)^3\tau}$	$\frac{m_0^2(m_0\alpha_m^2+\alpha w_0(4\alpha_m-3\alpha)}{(\alpha w_0+\alpha_m m_0)^3\tau}$
F	$\alpha\tau$	$\frac{-m_0\alpha\tau}{w_0}$	$\frac{-3m_0^2\alpha\tau}{w_0^2}$
G	w_{opt}	$\frac{-m_0w_{opt}}{w_0}$	$\frac{-3m_0^2w_{opt}}{w_0^2}$

Control	Time coefficient of $\langle \xi_w^2 \rangle$	Time coefficient of $\langle \xi_w \xi_m \rangle$	Time coefficient of $\langle \xi_m^2 \rangle$
A	$\frac{2m_0w_0(m_0+w_0)w_{opt}\alpha(1+(\alpha-1)\gamma)^2}{(m_0+w_0\alpha+m_0(\alpha-1)\gamma)^3\tau}$	$\frac{-2m_0w_0(m_0+w_0)w_{opt}\alpha^2(1+(\alpha-1)\gamma)}{(m_0+w_0\alpha+m_0(\alpha-1)\gamma)^3\tau}$	$\frac{2m_0w_0(m_0+w_0)w_{opt}\alpha^3}{(m_0+w_0\alpha+m_0(\alpha-1)\gamma)^3\tau}$
B	0	0	$\frac{2m_0(m_0+w_0)(w_{opt}\alpha\tau-1)}{w_0^2\alpha\tau^2}$
C	0	0	$\frac{2m_0(m_0+w_0)w_{opt}\alpha}{w_0^2(1+\alpha\tau)}$
D	$2w_0/\tau$	0	$2m_0/\tau$
E	$\frac{2m_0w_0(m_0+w_0)\alpha_m^2(w_{opt}\alpha\tau-1)}{(w_0\alpha+m_0\alpha_m)^3\tau^2}$	$\frac{-2m_0w_0(m_0+w_0)\alpha\alpha_m(w_{opt}\alpha\tau-1)}{(w_0\alpha+m_0\alpha_m)^3\tau^2}$	$\frac{2m_0w_0(m_0+w_0)\alpha^2(w_{opt}\alpha\tau-1)}{(w_0\alpha+m_0\alpha_m)^3\tau^2}$
F	0	0	$\frac{2m_0(m_0+w_0)\alpha}{w_0^2}$
G	0	0	$\frac{2m_0(m_0+w_0)w_{opt}}{w_0^2\tau}$

Control	Time coefficient of $\langle h^2 \rangle$ increase
A	$\frac{2m_0w_0(\alpha w_0+m_0+\gamma(\alpha-1)m_0)}{(m_0+w_0)^3w_{opt}\alpha\tau}$
B	$\frac{2m_0w_0^2\alpha}{(m_0+w_0)^3(w_{opt}\alpha\tau-1)}$
C	$\frac{2m_0w_0^2(1+\alpha\tau)}{(m_0+w_0)^3w_{opt}\alpha\tau^2}$
D	$\frac{2m_0w_0}{(m_0+w_0)^3\tau}$
E	$\frac{2m_0w_0(w_0\alpha+m_0\alpha_m)}{(m_0+w_0)^3(w_{opt}\alpha\tau-1)}$
F	$\frac{2m_0w_0^2}{(m_0+w_0)^3\alpha\tau^2}$
G	$\frac{2m_0w_0^2}{(m_0+w_0)^3w_{opt}\tau}$

Table S2: **Post-transient time behaviour of copy number and heteroplasmy variances in control strategies A-G.**

References

[1] N. Van Kampen. *Stochastic processes in physics and chemistry*, volume 1. 1992.

[2] J. Elf and M. Ehrenberg. Fast evaluation of fluctuations in biochemical networks with the linear noise approximation. *Genome Res.*, 13:2475, 2003.

[3] I. Johnston, J. Burgstaller, V. Havlicek, T. Kolbe, T. Rülicke, G. Brem, J. Poulton, and N. Jones. Stochastic modelling, Bayesian inference, and new in vivo measurements elucidate the debated mtDNA bottleneck mechanism. *eLife*, 4, 2015.

[4] I. Johnston and N. Jones. Closed-form stochastic solutions for non-equilibrium dynamics and inheritance of cellular components over many cell divisions. *Proc. Roy. Soc. A.*, 471, 2015.

[5] J. Burgstaller, I. Johnston, and J. Poulton. Mitochondrial DNA disease and developmental implications for reproductive strategies. *Mol. Hum. Reprod.*, 21:11, 2015.

[6] R. Rossignol, B. Faustin, C. Rocher, M. Malgat, J. Mazat, and T. Letellier. Mitochondrial threshold effects. *Biochem. J*, 370:751, 2003.

[7] J. Jenuth, A. Peterson, and E. Shoubridge. Tissue-specific selection for different mtdna genotypes in heteroplasmic mice. *Nature Genet.*, 16:93, 1997.

[8] J. Burgstaller, I. Johnston, N. Jones, J. Albrechtova, T. Kolbe, C. Vogl, A. Futschik, C. Mayrhofer, D. Klein, S. Sabitzer, M. Blattner, C. Gülly, J. Poulton, T. Rülicke, J. Piálek, R. Steinborn, and G. Brem. mtDNA segregation in heteroplasmic tissues is common in vivo and modulated by haplotype differences and developmental stage. *Cell Reports*, 7:2031, 2014.

[9] R. Jokinen, P. Marttinen, H. Sandell, T. Manninen, H. Teerenhovi, T. Wai, D. Teoli, J. Loredo-Osti, E. Shoubridge, and B. Battersby. Gimap3 regulates tissue-specific mitochondrial DNA segregation. *PLoS Genet.*, 6:e1001161, 2010.

[10] J. St John. The control of mtDNA replication during differentiation and development. *BBA*, 1840:1345, 2014.

[11] T. Toni, D. Welch, N. Strelkowa, A. Ipsen, and M. Stumpf. Approximate Bayesian computation scheme for parameter inference and model selection in dynamical systems. *J. Roy. Soc. Interf.*, 6:187, 2009.

[12] I. Johnston. Efficient parametric inference for stochastic biological systems with measured variability. *Stat. Appl. Genet. Mol. Biol.*, 13:379, 2014.

[13] A. Pyle, R. Taylor, S. Durham, M. Deschauer, A. Schaefer, D. Samuels, and P. Chinnery. Depletion of mitochondrial dna in leucocytes harbouring the 3243a g mtdna mutation. *J. Med. Genet.*, 44:69, 2007.

[14] http://www.bio-rad.com/webroot/web/pdf/lsr/literature/4106212b.pdf.